

Falkner-Skan wedge flow of Maxwell fluid with mixed convection



By

Muhammad Farooq

Department of Mathematics
Quaid-i-Azam University
Islamabad, Pakistan
2012

Falkner-Skan wedge flow of Maxwell fluid with mixed convection



By

Muhammad Farooq

Supervised By

Prof. Dr. Tasawar Hayat

Department of Mathematics
Quaid-i-Azam University
Islamabad, Pakistan
2012

Falkner-Skan wedge flow of Maxwell fluid with mixed convection



By
Muhammad Farooq

A Dissertation Submitted in the Partial Fulfillment of the Requirements for the
Degree of
MASTER OF PHILOSOPHY
IN
MATHEMATICS

Supervised By
Prof. Dr. Tasawar Hayat

Department of Mathematics
Quaid-i-Azam University
Islamabad, Pakistan
2012

Falkner-Skan wedge flow of Maxwell fluid with mixed convection


By


Muhammad Farooq


CERTIFICATE

A DISSERTATION SUBMITTED IN THE PARTIAL FULFILLMENT OF THE
REQUIREMENTS FOR THE DEGREE OF THE MASTER OF
PHILOSOPHY

We accept this dissertation as conforming to the required standard

1. 
Prof. Dr. Muhammad Ayub
(Chairman)

2. 
Prof. Dr. Tasawar Hayat
(Supervisor)

3. 
Prof. Dr. Saleem Asghar
(External Examiner)

Department of Mathematics
Quaid-i-Azam University
Islamabad, Pakistan
2012

DEDICATED TO

MY BELOVED PARENTS

AND

MY SUPERVISOR

Acknowledgement

In the name of **Allah** the beneficent and the most merciful, who granted me ability and potential to fulfill the requirements of my thesis. I offer my humblest gratitude to the **Holy Prophet Muahmmad (S. A. W)**, who is the source of knowledge and guidance to humanity.

I express deepest gratitude to my respected, affectionate and devoted supervisor **Prof. Dr. Tasawar Hayat** for his intellectual guidance, constant encouragement, suggestions and inexhaustible inspiration throughout my research work.

I am extremely thankful to **Prof. Dr. Muhammad Ayub** (Chairman, department of mathematics) for providing me opportunity to learn and seek knowledge in educated environment.

I am very thankful to my loving parents for their guidance, support and encouragement. I owe my heartiest gratitude for their assistance and never ending prayers for my success. I highly commend the cooperative behavior of my brothers (Haji Salim Khan, Haji Rafi ullah and Sami ullah), sisters and bhabhi who endeavored for my edification and betterment.

I would like to express my gratitude to respected teacher Hafiz Ikram ullah, cousins (Haji Irfan ullah, Haji Ikram ullah and Taus Khan) and friends Ismail, Zahid, Ejaz, Usman and Ilyas for their encouragement and special prayers.

I am also thankful to my respectable senior Zahid for their cooperation and suggestions throughout the research work.

I wish to express my special thanks to my friends and class fellows Shafqat, Ramzan, Jam, Taimoor, Masood, Qaiser, Zafar, Tayyab, Farhan, Waqar and Shah Jahan whose company made my stay in university full of joys with everlasting memories.

Muhammad Farooq

Preface

The dynamics of fluids with complex microstructure provide a major challenge to the researchers. Examples of such fluids include polymers, pasty materials, ketchup, mud, cheese, emulsions, certain oils, paints etc. The starting point for the description of most complex viscoelastic material is the consideration of a non-Newtonian fluid model. Many non-Newtonian fluid models exist due to diverse characteristics of complex fluids in nature [1-4]. Certainly, the non-Newtonian fluid models provide a more complicated expression of the apparent viscosity. The classical Navier-Stokes equations are inadequate for the description of such complex viscoelastic materials. Hence, several constitutive equations of non-Newtonian fluids have been proposed. In view of this, the non-Newtonian fluids have been mainly classified into three categories namely (i) the differential type, (ii) the rate type and (iii) the integral type. It is revealed from the literature that the boundary layer flows of rate type fluids have not been studied much when compared with the differential type fluids. In recent times, the boundary layer flow analysis of simplest subclass of rate type fluids (known as the upper-convected Maxwell (UCM) fluid) has been discussed [5, 6]. Further, the analysis of Falkner-Skan flow represents a fundamental problem in fluid mechanics. The description of previous studies through analytic and numerical treatments on this flow can be seen in the studies [7-9].

Now a days, the analysis of aerosol deposition is very significant in the engineering processes. Specifically, the contaminant particle deposition onto the surface of products in the electronic industry has a pivotal role regarding the quality of final product. Convection is one of the important factors that greatly influence particle deposition. Mixed convection flows are encountered in many engineering and industrial applications. Such flows widely occur in electronic devices cooled by fans, nuclear reactors cooled during emergency shutdown, heat exchanges placed in a low-velocity environment, flows in the ocean and in the atmosphere etc. Mixed convection due to moving surfaces also has applications in material processing systems including welding extrusion of plastics, hot rolling, paper drawing etc. A host of recent researchers [10-14] have contributed towards the analysis of boundary layer mixed convection past through the different

physical structures. In view of the above discussion the present dissertation is arranged as follows.

Chapter one includes some basic definitions and equations. Chapter two addresses the Falkner-Skan wedge flow of power law fluid with mixed convection and porous medium. Series solution of the developed problem is obtained by homotopy analysis method.

Chapter three describes Falkner-Skan wedge flow of Maxwell fluid with mixed convection. The present research extends the flow analysis of ref. [10] in two directions. We first consider the Maxwell fluid model. Second generalization is concerned with the examination of Newtonian heating. In fact there are four common heating processes which represent wall to ambient temperature distributions. When the heat transfer rate from the bounding surface with a finite heat capacity is proportional to the local surface temperature, the corresponding heating processes is known as Newtonian heating or conjugate convective flow [15]. The boundary layer flow and heat transfer over a stretching sheet with Newtonian heating is reported in the refs. [16-21]. This chapter is organized as follows. In section two we present the mathematical model of the problems. Section three contains series solution of the problems by homotopic approach [22-30]. Section four displays the convergence of the series solution. More, results and discussion are also included in this section. Some interesting points are noted in section five.

Contents

1	Basic definitions	4
1.1	Fluid	4
1.2	Fluid mechanics	4
1.2.1	Fluid statics	4
1.2.2	Fluid dynamic	5
1.3	Stress	5
1.3.1	Shear stress	5
1.3.2	Normal stress	5
1.4	Strain	5
1.5	Viscosity	5
1.5.1	Kinematic viscosity (ν)	6
1.6	Flow	6
1.6.1	Laminar flow	6
1.6.2	Turbulent flow	6
1.7	Newtonian's law of viscosity	6
1.8	Newtonian fluids	7
1.9	Non-Newtonian fluids	7
1.9.1	Rate type	8
1.10	Relaxation time	8
1.11	Retardation time	8
1.12	Porous medium	8
1.13	Mechanism of heat flow	8

1.13.1	Conduction	9
1.13.2	Convection	9
1.13.3	Radiation	9
1.14	Thermal conductivity	10
1.15	Thermal diffusivity	10
1.16	Newtonian heating	10
1.17	Dimensionless numbers	11
1.17.1	Reynold number	11
1.17.2	Prandtl number	11
1.17.3	Grashof number	12
1.17.4	Deborah number	12
1.17.5	Nusselt number	12
1.17.6	Skin friction	13
1.18	Falkner-Skan flow and transformation	13
1.19	Homotopy analysis method	14
2	Falkner-Skan wedge flow of power law fluid with mixed convection and porous medium	16
2.1	Introduction	16
2.2	Mathematical formulation	17
2.3	Solutions by the homotopy analysis method	20
2.3.1	Zeroth order problem	20
2.3.2	k th-order deformation problems	22
2.4	Analysis of the solutions	23
2.4.1	Convergence of the series solution	23
2.4.2	Discussion	25
2.5	Main points	37
3	Falkner-Skan wedge flow of Maxwell fluid with mixed convection	38
3.1	Introduction	38
3.2	Mathematical model	38

3.3	Solutions by homotopy analysis method (HAM)	43
3.3.1	Zeroth order problem	44
3.3.2	m th-order deformation problems	44
3.4	Solution analysis	46
3.4.1	Convergence of the series solutions	46
3.4.2	Result and discussion	46
3.5	Conclusions	53

Chapter 1

Basic definitions

This chapter consists of some fundamental definitions, concepts and laws which are useful for the understanding of analysis presented in the subsequent chapters.

1.1 Fluid

Fluid is a substance that deforms continuously under the influence of shear stress, no matter how small the shear stress may be or fluid is a substance which cannot sustain a shear force under the static condition.

1.2 Fluid mechanics

The branch of mechanics which concerns with the behavior of all fluids either at rest or in motion and also the effects of fluid properties on boundaries. In other words, fluid mechanics is a branch of continuous mechanics which describes the effects of forces on fluid particles in motion and under the static condition in a continuous material. It is divided into two main branches.

1.2.1 Fluid statics

It is the branch of fluid mechanics which describes the behavior of fluids under static condition (at rest).

1.2.2 Fluid dynamic

It is the branch of fluid mechanics which exhibits the behavior of fluids in motion.

1.3 Stress

The force acting on the surface of unit area within a deformable body is known as stress. The unit of stress in SI system is $kg/m.s^2$ and dimension $[\frac{M}{LT^2}]$. Further stress is divided into two following components.

1.3.1 Shear stress

In shear stress the force acts parallel to the unit surface area.

1.3.2 Normal stress

In normal stress the force acts perpendicular to the unit surface area.

1.4 Strain

Strain is a dimensionless quantity used to measure the deformation of an object caused by the applied forces.

1.5 Viscosity

It is the internal property of fluid that measures the resistance of a fluid against any deformation when different forces are acting upon it. Mathematically, it can be expressed as the ratio of shear stress to the rate of shear strain, i.e.

$$\text{viscosity } (\mu) = \frac{\text{shear stress}}{\text{rate of shear strain}}. \quad (1.1)$$

It is also known as absolute viscosity. Unit of viscosity in SI system is $kg/m.s$ and dimension $[\frac{M}{LT}]$.

1.5.1 Kinematic viscosity (ν)

The ratio of absolute viscosity μ to density of the fluid is known as kinematic viscosity. i.e.

$$\nu = \frac{\mu}{\rho}. \quad (1.2)$$

where μ is the absolute or dynamic viscosity and ρ is the density of the fluid. Its unit in SI system is m^2/s and dimension is $\left[\frac{L^2}{T}\right]$.

1.6 Flow

A material tends to deform under the influence of different forces. If the deformation increases continuously without any limit, then the phenomenon is known as flow.

1.6.1 Laminar flow

Laminar flow is that type of flow in which fluid particles have specific paths and paths of individual particles do not interact or cross each other. If we observe the smoke rising from a cigarette. For the first few centimeters the flow is certainly laminar. Then the smoke becomes turbulent.

1.6.2 Turbulent flow

Turbulent flow is that type of flow in which fluid particles have no specific paths and also these paths of individual particles cross each other.

1.7 Newtonian's law of viscosity

The Newton's law of viscosity states that shear stress which deforms the fluid element is directly and linearly proportional to velocity gradient.

Mathematically,

$$\tau_{yx} \propto \frac{du}{dy}, \quad (1.3)$$

or

$$\tau_{yx} = \mu \frac{du}{dy}. \quad (1.4)$$

where τ_{yx} is the shear stress acting on fluid element and μ is the constant of proportionality which is known as dynamic viscosity.

1.8 Newtonian fluids

Newtonian fluids are those which obey the Newton's law of viscosity i.e. shear stress is directly and linearly proportional to the deformation rate. It is noted that viscosity is constant for each Newtonian fluid at a given temperature and pressure. Examples of Newtonian fluids are water, sugar solutions, glycerin, light-hydrocarbon oils, silicone oils etc.

1.9 Non-Newtonian fluids

The fluids which do not obey the Newton's law of viscosity are known as the non-Newtonian fluids. It is noted that viscosity for such fluids do not remain constant but it changes with the applied shear stress. For such fluids we can write

$$\tau_{yx} \propto \left(\frac{du}{dy} \right)^n, \quad n \neq 1, \quad (1.5)$$

or

$$\tau_{yx} = \eta \frac{du}{dy}, \quad \eta = k \left(\frac{du}{dy} \right)^{n-1}. \quad (1.6)$$

where η is the apparent viscosity, k is the consistency index and n is the index of flow behavior. Noted that for $n = 1$ above equation reduces to the Newton's law of viscosity. Examples of such fluids are paints, flour dough, ketchup, polymer solutions, tooth paste and blood etc. Further non-Newtonian fluids are categorized into the three types (i) Integral type (ii) Differential type (iii) Rate type. In this dissertation we only consider the rate type fluids.

1.9.1 Rate type

Those fluids which characterize the relaxation and retardation time effects are known as rate type fluids. Examples of rate type fluids are Maxwell fluid, Oldroyd-B fluid and Burger's fluid etc.

1.10 Relaxation time

Under the influence of different forces a system goes to perturb. After removing such forces perturbed system return to its equilibrium. The time taken by the system to reach its equilibrium position from perturbed position is called relaxation time.

1.11 Retardation time

The time required to balance the applied shear stress by the opposing force produced in the fluid due to the applied shear stress is called retardation time.

1.12 Porous medium

A material which is composed of solid matrix with interconnected voids (pores) is called a porous medium. Fluid flows through these pores of a material and distribution of these pores are irregular in nature. Examples are sand, human lungs, human skin, sponge, filters, wood, paper and cloth etc.

1.13 Mechanism of heat flow

When one considers two different bodies located at different temperature then the heat flows from the body at high temperature to the body at low temperature. This transfer of heat takes place by three methods.

1.13.1 Conduction

The transfer of heat from one body to another body due to the only collision of molecules which are in contact and not due to the transfer of molecules is called conduction.

1.13.2 Convection

In this process the transfer of heat occurs due to the relative motion of molecules or transfer of molecules.

Forced convection

Forced convection is a mechanism of heat transfer in which fluid motion is generated by an external source like a pump and fan etc. Forced convection is typically used to increase the rate of heat exchange.

Natural convection

Natural convection occurs due to the temperature differences which effect the density and thus buoyancy of the fluid. Natural convection can only occur, when there is gravitational field. It is also known as free convection.

Mixed convection

Mixed convection flow occurs when both natural and forced convection processes simultaneously and significantly contribute to heat transfer.

1.13.3 Radiation

Radiation is that process in which heat is transferred directly by electromagnetic radiations.

In liquids and gases convection and radiation play very important role in the transfer of heat but in solids convection is totally absent and radiation is usually negligible. Thus for solid materials conduction play major role in the transfer of heat.

1.14 Thermal conductivity

It is the property of a material which measures the ability to conduct heat.

Fourier's law of conduction which relates the rate of heat transfer by conduction to the temperature gradient is

$$\frac{dQ}{dt} = -kA \frac{dT}{dx} \quad (1.7)$$

where $\frac{dQ}{dt}$ is the rate of heat transfer, k is the thermal conductivity, A is the area and $\frac{dT}{dx}$ is the temperature gradient.

Now we define the thermal conductivity from the Fourier's law as

"the rate of heat transfer through a unit thickness of a material per unit area and per unit temperature difference".

Thermal conductivity of most liquids decrease with increasing temperature except water. The unit of thermal conductivity is $kg.m/s^3.K$ and dimension is $[\frac{ML}{T^3\theta}]$.

1.15 Thermal diffusivity

Thermal diffusivity of a material is defined as, "thermal conductivity of a material divided by the product of density and specific heat at constant pressure".

Mathematically it can be expressed as

$$\alpha = \frac{k}{\rho c_p} \quad (1.8)$$

The unit of thermal diffusivity in SI system is m^2/s and dimension is $[\frac{L^2}{T}]$.

1.16 Newtonian heating

Newtonian heating is that type of heat transfer in which the internal resistance of a body to flow heat is neglected. In this process the rate of heat transfer is directly proportional to the surface temperature of the body. It is noted that in Newtonian heating the temperature remains same throughout the body at a given time. This type of analysis is also called as the lumped heat

1.17 Dimensionless numbers

1.17.1 Reynold number

Reynold number for the fluid behavior in the boundary layer is defined as, "the ratio of inertial forces to viscous forces". Inertial forces act upon all masses in a non-inertial frame of reference while viscous force is the internal resistance of a fluid to flow.

Mathematically it can be expressed as

$$\text{Re} = \frac{\text{Inertial force}}{\text{Viscous force}} \quad (1.9)$$

$$\text{Re} = \frac{\rho v^2 / L}{\mu v / L^2} \quad \Rightarrow \quad \text{Re} = \frac{Lv}{\nu} \quad (1.10)$$

where v is the fluid velocity, L is the characteristic length and ν is the kinematic viscosity. For small Reynold number viscous forces are dominant which characterize by the laminar flow while turbulent flow occurs at high Reynold number due to the dominant inertial forces.

1.17.2 Prandtl number

It is the dimensionless number which measures the ratio of momentum diffusivity to thermal diffusivity. Mathematically it can be written as

$$\text{Pr} = \frac{\text{viscous diffusion rate}}{\text{thermal diffusion rate}} \quad (1.11)$$

$$\text{Pr} = \frac{\nu}{\alpha} = \frac{\mu / \rho}{k / \rho c_p} = \frac{\mu c_p}{k} \quad (1.12)$$

where ν is the kinematic viscosity or momentum diffusivity and α is the thermal diffusivity. Physical significance of Prandtl number is that, it gives the relative thickness of velocity boundary layer and thermal boundary layer. For small Pr heat diffuses very quickly as compared to the momentum.

1.17.3 Grashof number

It describes the relationship between buoyancy force and viscous force acting on a fluid. It is named after the German engineer Franz Grashof.

Mathematically it can be represented by the relation,

$$Gr = g\beta(T - T_{\infty})\frac{L^3}{\nu^2} \quad (1.13)$$

where g is the gravitational acceleration, β is the volumetric thermal expansion coefficient, L is the characteristic length, ν is the kinematic viscosity and T, T_{∞} are the temperature of the fluid and surrounding respectively.

1.17.4 Deborah number

It is the ratio of time of relaxation to time of observation or characteristic time scale for a material. Mathematically it can be defined as

$$De = \frac{t_c}{t_p} \quad (1.14)$$

where t_c is the relaxation time and t_p is the characteristic time or time of observation. If the time of relaxation of a material is very small than the time of observation i.e. small Deborah number, material behaves like fluid with an associated Newtonian viscous flow. But on the other hand, if the time of relaxation of a material is large than the time of observation then material behaves like solid.

1.17.5 Nusselt number

It is the dimensionless heat transfer coefficient which gives a measure of the ratio of convective to conductive heat transfer across the boundary and can be expressed as

$$Nu_L = \frac{\text{convective heat transfer coefficient}}{\text{conductive heat transfer coefficient}} \quad (1.15)$$

Now heat transfer by convection is $(h\Delta T)$ and by conduction is $(k\Delta T/L)$. So Nusselt number becomes

$$Nu_L = \frac{h\Delta T}{k\Delta T/L} = \frac{hL}{k} \quad (1.16)$$

where h is the convective heat transfer, L is the characteristic length and k is the thermal conductivity of the fluid.

1.17.6 Skin friction

When fluid moves across a surface certain amount of friction appears which is called skin friction. It occurs between the fluid and the surface, which tends to slow the fluid's motion. The skin friction coefficient is defined as,

$$C_f = \frac{\tau_w}{\rho U^2/2} \quad (1.17)$$

where τ_w is the shear stress at the wall, ρ is the density and U is free-stream velocity.

1.18 Falkner-Skan flow and transformation

A class of self-similar boundary-layer flows in the presence of a pressure gradient was found by Falkner and Skan (1930). Falkner-Skan flow is an external flow with a pressure gradient. This type of flow is characterized by flow past wedge shaped bodies. We consider the boundary layer equations

$$\frac{\partial u}{\partial x} + \frac{\partial v}{\partial y} = 0 \quad (1.18)$$

$$u \frac{\partial u}{\partial x} + v \frac{\partial u}{\partial y} = -\frac{1}{\rho} \frac{\partial p}{\partial x} + \nu \frac{\partial^2 u}{\partial y^2} \quad (1.19)$$

where

$$-\frac{1}{\rho} \frac{\partial p}{\partial x} = U \frac{\partial U}{\partial x} \quad (1.20)$$

in which the free stream velocity U is proportional to x^m .

$$U \propto x^m \quad \text{or} \quad U = ax^m \quad (1.21)$$

where a is constant. Now for the Falkner-Skan flow we define the similarity variables of the form

$$\eta = y \sqrt{\frac{(m+1)}{2} \frac{U}{\nu x}} = y \sqrt{\frac{(m+1) C x^{m-1}}{2\nu}} \quad (1.22)$$

and

$$\psi = \sqrt{\frac{2\nu U x}{(m+1)}} f(\eta) = \sqrt{\frac{2\nu C x^{m+1}}{(m+1)}} f(\eta) \quad (1.23)$$

Using Eqs. (1.22) and (1.23) in (1.19) we get

$$f''' + f f'' + \beta (1 - f'^2) = 0 \quad (1.24)$$

with the boundary conditions

$$f(0) = f'(0) = 0, \quad f'(\infty) = 1 \quad (1.25)$$

where

$$\beta = \frac{2m}{m+1} \quad (1.26)$$

The expression (1.24) is known as Falkner-Skan equation. For $\beta = 0$, Eq. (1.24) reduces to the Blasius equation which gives the flat plate flow. For $\beta = 1$, it reduces to the stagnation point flow and $\beta = -0.1988$, for the separated flow. The parameter β denotes the behavior of pressure gradient. For positive values of the parameter β the pressure gradient is negative or favorable and if β is negative, the pressure gradient is positive or adverse. Further, for separated flow the value of β denotes the point where the pressure gradient is zero.

1.19 Homotopy analysis method

In order to solve the non-linear problems, Liao [22] proposed a method which is known as homotopy analysis method (HAM). For the basic idea of homotopy analysis method, we consider the following differential equation

$$N[u(x)] = 0, \quad (1.27)$$

where N is a non-linear operator, x is the independent variable and $u(x)$ is the unknown function. The zeroth-order deformation equation is

$$(1 - q) \mathcal{L} [\hat{u}(x; q) - u_0(x)] = q \hbar N [\hat{u}(x; q)], \quad (1.28)$$

in which $u_0(x)$ denotes the initial approximation, \mathcal{L} is the auxiliary linear operator, $q \in [0, 1]$ is an embedding parameter, \hbar is an auxiliary parameter and $\hat{u}(x; q)$ is unknown function of x and q .

For $q = 0$ and $q = 1$, One has

$$\hat{u}(x; 0) = u_0(x), \quad \text{and} \quad \hat{u}(x; 1) = u(x) \quad (1.29)$$

As when q varies from 0 to 1, the solution $\hat{u}(x; q)$ varies from initial approximation $u_0(x)$ to the final solution $u(x)$. By Taylor series expansion one can write

$$\hat{u}(x; q) = u_0(x) + \sum_{m=1}^{\infty} u_m(x) q^m, \quad u_m(x) = \frac{1}{m!} \left. \frac{\partial^m \hat{u}(x; q)}{\partial q^m} \right|_{q=0}. \quad (1.30)$$

when $q = 1$, we get

$$u(x) = u_0(x) + \sum_{m=1}^{\infty} u_m(x) \quad (1.31)$$

Differentiating the zeroth-order deformation Eq.(1.28) m -time with respect to q , then dividing by $m!$ and finally setting $q = 0$, we get the m -th order deformation equation

$$\mathcal{L} [u_m(x) - \chi_m u_{m-1}(x)] = \hbar \mathcal{R}_m(x), \quad (1.32)$$

$$\mathcal{R}_m(x) = \frac{1}{(m-1)!} \left. \frac{\partial^{m-1} N [\hat{u}(x; q)]}{\partial q^{m-1}} \right|_{q=0} \quad (1.33)$$

with

$$\chi_m = \begin{cases} 0, & m \leq 1 \\ 1, & m > 1 \end{cases}. \quad (1.34)$$

Chapter 2

Falkner-Skan wedge flow of power law fluid with mixed convection and porous medium

2.1 Introduction

Here an analytical solution is developed for a steady two-dimensional Falkner-Skan wedge flow of an incompressible power-law fluid. The effects of porous medium and heat transfer by mixed convection are examined. The energy equation in the present flow is also solved. The governing nonlinear partial differential equations are converted to the ordinary differential equations by suitable similarity transformations. The arising mathematical problems have been solved by homotopy analysis method (HAM). Convergence of problems have been checked. The influence of different parameters are presented through graphs and tabulated values. The numerical values of local Nusselt number and skin friction coefficient are computed and analyzed. The work in this chapter is a review of research paper [10].

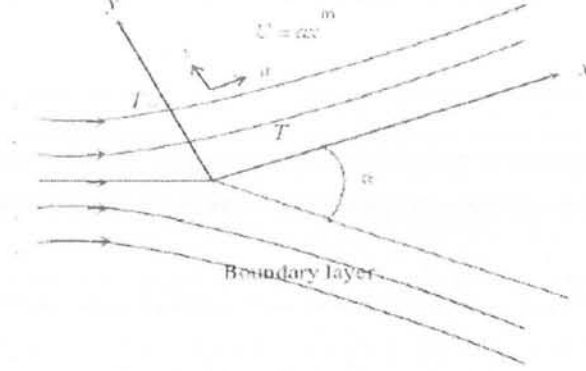


Fig. 1. Physical flow model.

2.2 Mathematical formulation

Consider the two-dimensional Falkner-Skan wedge flow and heat transfer of a power-law fluid under the influence of mixed convection. Further fluid saturates the porous medium. Cartesian coordinates (x, y) are used in which x -axis is parallel to the plate and y -axis perpendicular to it. The continuity and momentum equations are

$$\nabla \cdot \mathbf{V} = 0, \quad (2.1)$$

$$\rho a = \nabla \cdot \mathbf{T} + R, \quad (2.2)$$

The velocity field for the present flow is

$$\mathbf{V} = [u(x, y), v(x, y), 0]. \quad (2.3)$$

By invoking velocity field in Eqs. (2.1) and (2.2), the boundary layer equations governing the flow in a power-law fluid are

$$\frac{\partial u}{\partial x} + \frac{\partial v}{\partial y} = 0, \quad (2.4)$$

$$u \frac{\partial u}{\partial x} + v \frac{\partial u}{\partial y} = -\frac{1}{\rho} \frac{\partial p}{\partial x} + \frac{1}{\rho} \frac{\partial \tau_{xy}}{\partial y} + \frac{1}{\rho} R_x. \quad (2.5)$$

The stress tensor for the power-law model is

$$\tau_{ij} = 2\mu |2D_{kl}D_{kl}|^{\frac{n-1}{2}} D_{ij} \quad (2.6)$$

and

$$D_{ij} = \frac{1}{2} \left(\frac{\partial u_i}{\partial x_j} + \frac{\partial u_j}{\partial x_i} \right) \quad (2.7)$$

where D_{ij} denotes the stretching tensor, n is the power-law index, μ is the consistency coefficient of viscosity. R_x is the flow resistance offered by the porous medium given by

$$R_x = -\frac{\mu\epsilon}{K} u^n - \frac{\rho F \epsilon^2}{\sqrt{K}} u^2 \quad (2.8)$$

Using Eqs. (2.6 – 2.8) in Eq. (2.5) we obtain

$$u \frac{\partial u}{\partial x} + v \frac{\partial u}{\partial y} = -\frac{1}{\rho} \frac{\partial p}{\partial x} + \frac{1}{\rho} \frac{\partial}{\partial y} \left(\mu \left| \frac{\partial u}{\partial y} \right|^n \right) - \frac{\mu\epsilon}{\rho K} u^n - \frac{F \epsilon^2}{\sqrt{K}} u^2 \quad (2.9)$$

In the presence of buoyancy forces Eq. (2.9) becomes

$$u \frac{\partial u}{\partial x} + v \frac{\partial u}{\partial y} = -\frac{1}{\rho} \frac{\partial p}{\partial x} + \frac{1}{\rho} \frac{\partial}{\partial y} \left(\mu \left| \frac{\partial u}{\partial y} \right|^n \right) - \frac{\mu\epsilon}{\rho K} u^n - \frac{F \epsilon^2}{\sqrt{K}} u^2 + g_c \beta_T (T - T_\infty) \sin \left(\frac{\alpha}{2} \right) \quad (2.10)$$

In the above expressions u and v are the velocity components in the x and y -direction, n is the power law index, ρ is the density, ϵ is the medium porosity, K is the permeability parameter of the porous medium, F is the imperial constant in the second order resistance, β_T is the thermal expansion coefficient and α is the angle of inclination.

The energy equation for the present problem is

$$\rho c_p \frac{dT}{dt} = \mathbf{T} \cdot \mathbf{L} - \text{div } \mathbf{q}, \quad (2.11)$$

$$\mathbf{q} = -k_0 \text{grad } T, \quad (2.12)$$

where ρ is the density of fluid, c_p is the specific heat, \mathbf{T} is the Cauchy stress tensor, \mathbf{L} is the velocity gradient, T is the temperature, \mathbf{q} is the heat flux and k_0 is the thermal conductivity.

Eq. (2.11) in the absence of viscous dissipation becomes

$$\rho c_p \left(u \frac{\partial T}{\partial x} + v \frac{\partial T}{\partial y} \right) = k_0 \frac{\partial^2 T}{\partial y^2}. \quad (2.13)$$

The subjected boundary conditions are

$$\begin{aligned} u &= 0, & v &= 0, & T &= T_w & \text{at } y = 0, \\ u &\rightarrow U, & v &\rightarrow 0 & T &\rightarrow T_\infty & \text{as } y \rightarrow \infty. \end{aligned} \quad (2.14)$$

Here $U (=cx^m)$ is the free stream velocity. The relation between the Falkner-Skan power law parameter and wedge angle $\beta\pi$ is

$$\beta = \frac{2m}{1+m} \quad (2.15)$$

Noted that U increases along the wedge surface when $\beta > 0$ and decreases for $\beta < 0$.

We define the similarity transformation of the form

$$\begin{aligned} \eta &= yg(x) = \frac{y}{x} \text{Re}_x^{\frac{1}{n+1}}, & \psi &= U(x) x \text{Re}_x^{\frac{-1}{n+1}} f(\eta) \\ \text{Re}_x &= (m+1) \frac{\rho x^n U(x)^{2-n}}{\mu}, \end{aligned} \quad (2.16)$$

$$v = -U(x) \text{Re}_x^{-\frac{1}{n+1}} \frac{1}{n+1} \{ [m(2n-1)+1] f + [m(2-n)-1] \eta f' \}, \quad u = U(x) f'. \quad (2.17)$$

Using Eqs. (2.16) and (2.17) into Eqs. (2.4), (2.10), (2.13) and (2.14), it is noted that Eq. (2.4) is identically satisfied while Eqs.(2.10), (2.13) and (2.14) are reduced as follows

$$n |f''|^{n-1} f''' + \frac{m(2n-1)+1}{(m+1)(n+1)} f f'' + \frac{B}{m+1} - \frac{B-m}{m+1} f'^2 + \frac{A}{m+1} [1 - (f')^n] + \lambda \theta \text{Si } n \left(\frac{\alpha}{2} \right) = 0, \quad (2.18)$$

$$\theta'' + \frac{[m(2n-1)+1]}{n+1} \text{Pr } f \theta' = 0, \quad (2.19)$$

$$\begin{aligned} f &= f' = 0, & \theta &= 1, & \text{at } \eta &= 0, \\ f' &= 1, & \theta &\rightarrow 0 & \text{as } \eta &\rightarrow \infty, \end{aligned} \quad (2.20)$$

where

$$A = \frac{\mu \epsilon}{\rho K} x U^{n-2}, \quad B = \frac{F \epsilon^2}{\sqrt{K}} x, \quad \lambda = \frac{Gr_x}{Re_x^2}, \quad Pr = \frac{x U Re_x^{\frac{-2}{n+1}}}{\alpha}, \quad (2.21)$$

$$Gr_x = (m+1) g_c \beta_T (T_w - T_\infty) \frac{x^{1+2n}}{v^2} U^{2(1-n)}, \quad Re = (m+1) \frac{x^n}{\nu} U^{2-n}. \quad (2.22)$$

The skin friction coefficient and the local Nusselt number are defined as

$$C_f = \frac{\tau_{xy}(0)}{\rho U^2/2}, \quad \text{and} \quad Nu_x = \frac{x q_w}{k_0 (T - T_\infty)}, \quad (2.23)$$

with

$$\tau_{xy} = \mu \left(\frac{\partial u}{\partial y} \right)_{y=0}^n, \quad q_w = -k_0 \left(\frac{\partial T}{\partial y} \right)_{y=0}. \quad (2.24)$$

Using similarity transformations in Eqs. (2.23) and (2.24) we get

$$\frac{1}{2} C_f Re_x^{\frac{1}{n+1}} = (m+1) |f''(0)|^n, \quad Nu_x Re_x^{\frac{-1}{n+1}} = -\theta'(0). \quad (2.25)$$

2.3 Solutions by the homotopy analysis method

As we know that the homotopy solutions depend on the initial guesses (f_0, θ_0) and auxiliary linear operators (L_f, L_θ) which are chosen in the forms

$$f_0 = \eta - 1 + \text{Exp}(-\eta), \quad \theta_0 = \text{Exp}(-\eta), \quad (2.26)$$

$$\mathcal{L}_f[f(\eta)] = \frac{\partial^3 f}{\partial \eta^3} - \frac{\partial f}{\partial \eta}, \quad \mathcal{L}_\theta[\theta(\eta)] = \frac{\partial^2 \theta}{\partial \eta^2} - \theta, \quad (2.27)$$

with the properties

$$\mathcal{L}_f[A_1 e^{-\eta} + A_2 e^\eta + A_3] = 0, \quad (2.28)$$

$$\mathcal{L}_\theta[A_4 e^{-\eta} + A_5 e^\eta] = 0, \quad (2.29)$$

where A_i ($i = 1 - 5$) are the arbitrary constants.

2.3.1 Zeroth order problem

$$(1 - q) \mathcal{L}_f[\hat{f}(\eta; q) - f_0(\eta)] = q \hbar_f \mathcal{N}_f[\hat{f}(\eta; q)], \quad (2.30)$$

$$(1 - q) \mathcal{L}_\theta [\theta(\eta; q) - \theta_0(\eta)] = q \hbar_\theta \mathcal{N}_\theta [\theta(\eta; q)], \quad (2.31)$$

$$\widehat{f}(0; q) = \frac{\partial f(0; q)}{\partial \eta} = 0, \quad \theta(0; q) = 1, \eta = 0, \quad (2.32)$$

$$\frac{\partial \widehat{f}(\eta)}{\partial \eta} = 1, \quad \theta(\eta) \rightarrow 0 \quad \text{as } \eta \rightarrow \infty, \quad (2.33)$$

where \hbar_f and \hbar_θ are the non-zero auxiliary parameters, $q \in [0, 1]$ is the embedding parameter and the nonlinear operators \mathcal{N}_f and \mathcal{N}_θ are

$$\begin{aligned} \mathcal{N}_f [\widehat{f}(\eta, q)] &= n \left[\frac{\partial^2 f}{\partial \eta^2} \right]^{n-1} \frac{\partial^3 f}{\partial \eta^3} + \frac{m(2n-1)+1}{(m+1)(n+1)} f \frac{\partial^2 f}{\partial \eta^2} + \frac{B}{m+1} - \frac{(B-m)}{(m+1)} \left(\frac{\partial f}{\partial \eta} \right)^2 \\ &+ \frac{A}{m+1} \left[1 - \left(\frac{\partial f}{\partial \eta} \right)^n \right] + \lambda \theta \operatorname{Si} n \left(\frac{\alpha}{2} \right), \end{aligned} \quad (2.34)$$

$$\mathcal{N}_\theta [\theta(\eta; q)] = \frac{\partial^2 \theta}{\partial \eta^2} + \frac{1}{n+1} \operatorname{Pr} [m(2n-1)+1] f \frac{\partial \theta}{\partial \eta}, \quad (2.35)$$

$$\widehat{f}(\eta, 0) = f_0(\eta), \quad \widehat{\theta}(\eta, 0) = \theta_0(\eta), \quad (2.36)$$

$$\widehat{f}(\eta, 1) = f(\eta), \quad \widehat{\theta}(\eta, 1) = \theta(\eta), \quad (2.37)$$

when q varies from 0 to 1 then $\widehat{f}(\eta, q)$ and $\widehat{\theta}(\eta, q)$ vary from the initial guesses $f_0(\eta)$ and $\theta_0(\eta)$ to the final solutions $f(\eta)$ and $g(\eta)$ respectively. Expanding $\widehat{f}(\eta, q)$ and $\widehat{\theta}(\eta, q)$ in Taylor's series with respect to the embedding parameter q one can write

$$\widehat{f}(\eta, q) = f_0(\eta) + \sum_{k=1}^{\infty} f_k(\eta) q^k, \quad f_k(\eta) = \frac{1}{k!} \frac{\partial^k \widehat{f}(\eta, q)}{\partial q^k} \Big|_{q=0}, \quad (2.38)$$

$$\widehat{\theta}(\eta, q) = \theta_0(\eta) + \sum_{k=1}^{\infty} \theta_k(\eta) q^k, \quad \theta_k(\eta) = \frac{1}{k!} \frac{\partial^k \widehat{\theta}(\eta, q)}{\partial q^k} \Big|_{q=0}. \quad (2.39)$$

The auxiliary parameters \hbar_f and \hbar_θ are so properly chosen that the series (2.38) and (2.39) converge at $q = 1$. Hence we have

$$f(\eta) = f_0(\eta) + \sum_{k=1}^{\infty} f_k(\eta), \quad (2.40)$$

$$\theta(\eta) = \theta_0(\eta) + \sum_{k=1}^{\infty} \theta_k(\eta). \quad (2.41)$$

2.3.2 k th-order deformation problems

Differentiating the zeroth-order deformation problem (2.30) and (2.31) k -times with respect to q , dividing by $k!$ and setting $q = 0$, the k th-order deformation problem is given by

$$\mathcal{L}_f [f_k(\eta) - \chi_k f_{k-1}(\eta)] = \hbar_f \mathcal{R}_{f,k}(\eta), \quad (2.42)$$

$$\mathcal{L}_\theta [\theta_k(\eta) - \chi_k \theta_{k-1}(\eta)] = \hbar_\theta \mathcal{R}_{\theta,k}(\eta), \quad (2.43)$$

$$f_k(0) = 0, \quad f'_k(0) = 0, \quad \theta_k(0) = 0, \quad (2.44)$$

$$f'_k(\eta) = 0, \quad \theta_k(\eta) = 0, \quad \text{as } \eta \rightarrow \infty. \quad (2.45)$$

When $n = 1$ the nonlinear operators are

$$\begin{aligned} \mathcal{R}_k^f(\eta) = & \frac{\partial^3 f_{k-1}}{\partial \eta^3} + \frac{1}{2} \sum_{i=0}^{k-1} f_i \frac{\partial^2 f_{k-i-1}}{\partial \eta^2} - \frac{(B-m)}{m+1} \sum_{i=0}^{k-1} \frac{\partial f_i}{\partial \eta} \frac{\partial f_{k-i-1}}{\partial \eta} \\ & - \frac{A}{m+1} \frac{\partial f_{k-1}}{\partial \eta} + \lambda \theta_{k-1} \text{Si} n \left(\frac{\alpha}{2} \right) + \left(\frac{A}{m+1} + \frac{B}{m+1} \right) (1 - \chi_k), \end{aligned} \quad (2.46)$$

$$\mathcal{R}_k^\theta(\eta) = \frac{\partial^2 \theta_{k-1}}{\partial \eta^2} + \frac{[m(2n-1)+1]}{n+1} \text{Pr} \sum_{i=0}^{k-1} f_i \frac{\partial \theta_{k-i-1}}{\partial \eta}. \quad (2.47)$$

The non linear operators for $n = 2$ are given by

$$\begin{aligned} \mathcal{R}_k^f(\eta) = & 2 \sum_{i=0}^{k-1} \frac{\partial^2 f_i}{\partial \eta^2} \frac{\partial^3 f_{k-i-1}}{\partial \eta^3} + \frac{3m+1}{4(m+1)} \sum_{i=0}^{k-1} f_i \frac{\partial^2 f_{k-i-1}}{\partial \eta^2} - \frac{(B-m)}{m+1} \sum_{i=0}^{k-1} \frac{\partial f_i}{\partial \eta} \frac{\partial f_{k-i-1}}{\partial \eta} \\ & - \frac{A}{m+1} \sum_{i=0}^{k-1} \frac{\partial f_i}{\partial \eta} \frac{\partial f_{k-i-1}}{\partial \eta} + \lambda \theta_{k-1} \text{Si} n \left(\frac{\alpha}{2} \right) + \left(\frac{A}{m+1} + \frac{B}{m+1} \right) (1 - \chi_k) \end{aligned} \quad (2.48)$$

$$\mathcal{R}_k^\theta(\eta) = \frac{\partial^2 \theta_{k-1}}{\partial \eta^2} + \frac{1}{3} \text{Pr} [3m+1] \sum_{i=0}^{k-1} f_i \frac{\partial \theta_{k-i-1}}{\partial \eta} \quad (2.49)$$

and similarly we can obtain for $n = 3, 4, \dots$

with

$$\chi_k = \begin{cases} 0, & k \leq 1 \\ 1, & k > 1 \end{cases} \quad (2.50)$$

The general solutions of Eqs. (2.42) and (2.43) can be written as

$$f_k(\eta) = f_k^*(\eta) + A_1 + A_2 e^\eta + A_3 e^{-\eta}, \quad (2.51)$$

$$\theta_k(\eta) = \theta_k^*(\eta) + A_4 e^\eta + A_5 e^{-\eta}, \quad (2.52)$$

in which f_k^* and θ_k^* are the special solutions and the values of A_i ($i = 1 - 5$) after using the boundary conditions (2.44) and (2.45) are given by

$$\begin{aligned} A_2 &= A_4 = 0, & A_3 &= \left. \frac{\partial f_k^*(\eta)}{\partial \eta} \right|_{\eta=0}, & A_1 &= -A_3 - f_k^*(0), \\ A_5 &= \theta_k^*(\eta)|_{\eta=0}, \end{aligned} \quad (2.53)$$

Note that the solutions of the problems involving Eqs. (2.42) – (2.50) are constructed using the symbolic computation software MATHEMATICA when $k = 1, 2, 3, \dots$.

2.4 Analysis of the solutions

2.4.1 Convergence of the series solution

We know that the series solutions contain auxiliary parameters \hbar_f and \hbar_θ . The convergence of series solutions depend upon these parameters. The relevant \hbar -curves have been sketched in the Figs. 1 and 2. It is noticed that the admissible ranges of \hbar_f and \hbar_θ are $-1.5 \leq \hbar_f \leq -0.5$ and $-1.6 \leq \hbar_\theta \leq -0.4$.

Table 2.1 : Convergence of the series solutions for different order of approximation when $A = 0.1, B = 0.1, m = 1, \lambda = 1, Pr = 1$ and $\alpha = \pi/4$.

Order of approximation	$-f'''(0)$	$\theta''(0)$
1	0.39314	0.20000
3	0.24749	0.0080000
6	0.24147	0.000064000
8	0.24142	0.0000025600
9	0.24142	0.0000025600
15	0.24142	0.0000025600

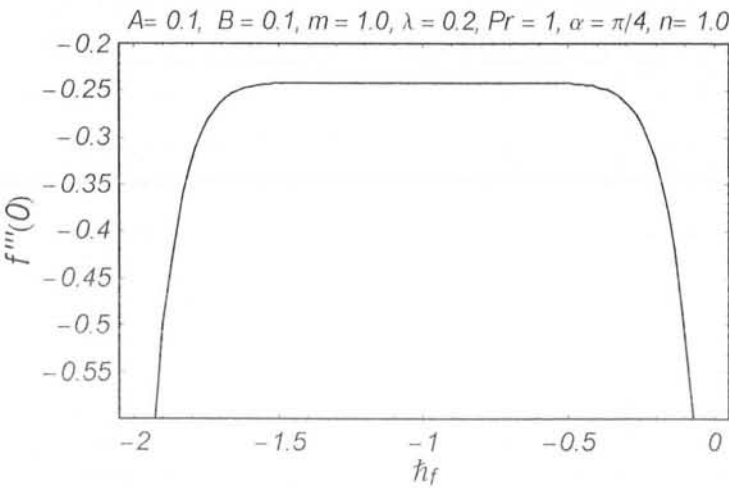


Fig. 2.2. h -curve for the function f .

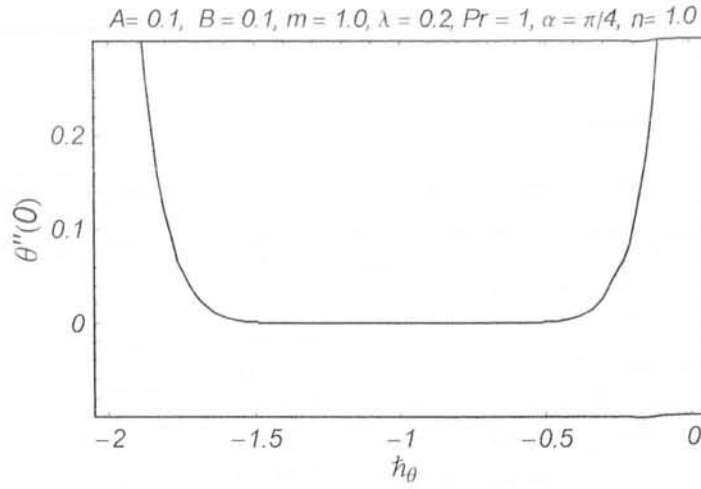


Fig. 2.3. \hbar -curve for the function θ .

2.4.2 Discussion

In this section we study the effects of different embedded parameters on the velocity and temperature profiles. Therefore, Figs. 2.4 – 2.21 have been prepared. Figs. 2.4 – 2.6 indicate the effect of A on the velocity profile for the different values of m and $n = 1$. It is observed that the velocity profile increases with increase in A but the velocity field increases slowly by increasing m . The velocity boundary layer thickness decreases with an increase in A . However, it gives opposite behavior for λ which can be seen in the Figs. 2.7 – 2.9. These Figs. show that the velocity profile increases with an increase in the values of λ . Further, the velocity field increases largely when m increases and velocity boundary layer thickness decreases. The effect of A on velocity profile is plotted in the Figs. 2.10 – 2.12 for the different values of m and $n = 2$. It is observed that the velocity profile increases with an increase in the values of A but the velocity profile increases slowly when m is increased. From these Figs. we also observed that the velocity boundary layer thickness decreases. The effect of λ on the velocity profile is sketched in the Figs. 2.13 – 2.15 for different values of m . It is noticed that an increase in the values of λ yields an increase in the velocity profile. However, the velocity boundary layer thickness decreases. The effect of Prandtl number on temperature profile is shown in the Figs. 2.16 – 2.18 for different values of m and $n = 1$. It is clear that temperature profile decreases with an increase of Pr . Further thermal boundary layer thickness decreases and it is also observed

that temperature profile decreases largely by increasing m . Figs. (2.19 – 2.21) are plotted the effect of Pr on temperature profile for the different values of m and $n = 2$. It is observed that the temperature profile decreases with an increase in Pr and thermal boundary layer thickness decreases. Further, the temperature profile decreases largely when m increases.

Table 2 and 3 show the effects of $(m + 1) f''(0)$ and $(-\theta'(0))$ for different values of parameters. The magnitude of skin friction coefficient increases with the increase in m , A , B , λ and α . Local nusselt number increases with an increase in m , n and Pr .

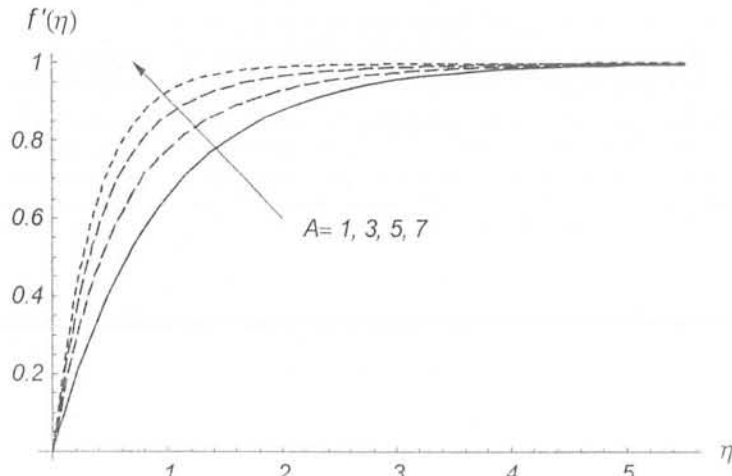


Fig. 2.4. Effect of A on f' for $n = 1$ and $m = 0$.

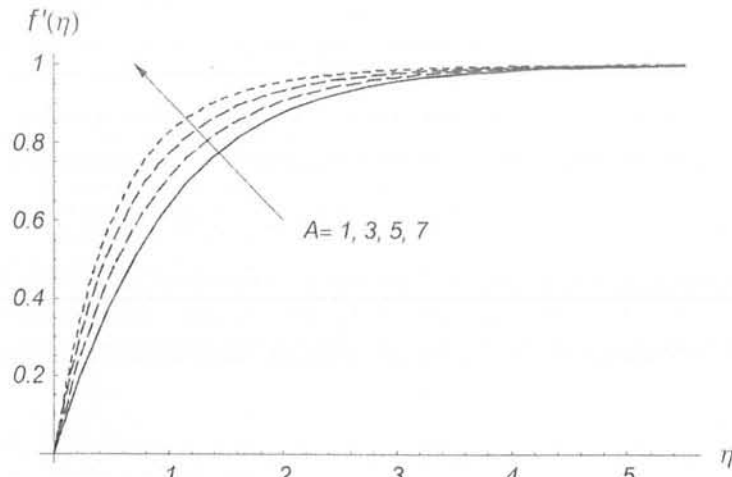


Fig. 2.5. Effect of A on f' for $n = 1$ and $m = 1$.

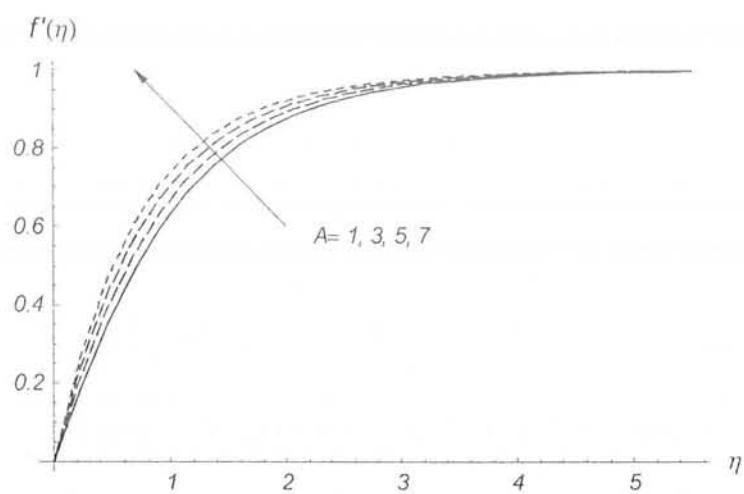


Fig. 2.6. Effect of A on f' for $n = 1$ and $m = 3$.

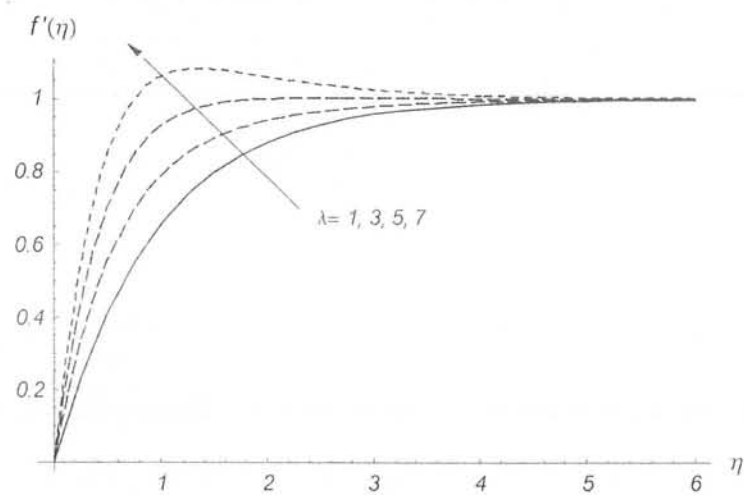


Fig. 2.7. Effect of λ on f' for $n = 1$ and $m = 0.3$.

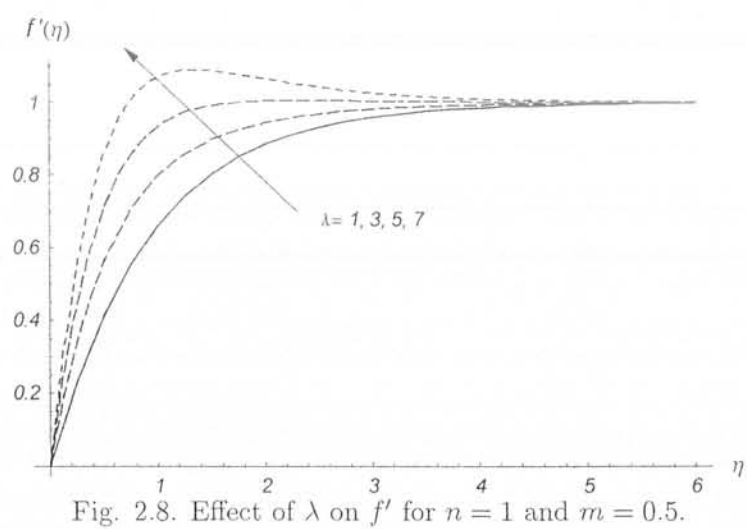


Fig. 2.8. Effect of λ on f' for $n = 1$ and $m = 0.5$.

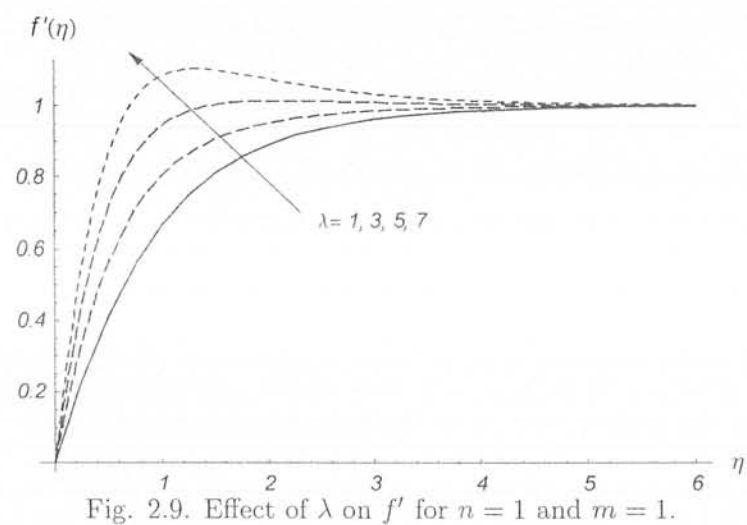


Fig. 2.9. Effect of λ on f' for $n = 1$ and $m = 1$.

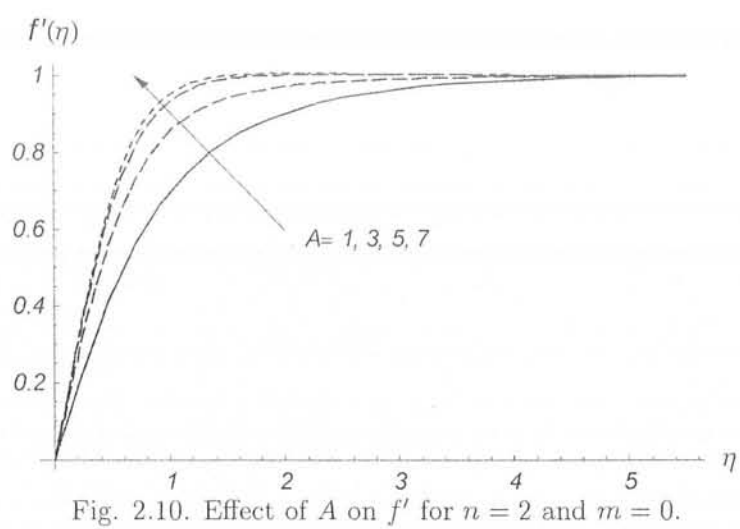


Fig. 2.10. Effect of A on f' for $n = 2$ and $m = 0$.

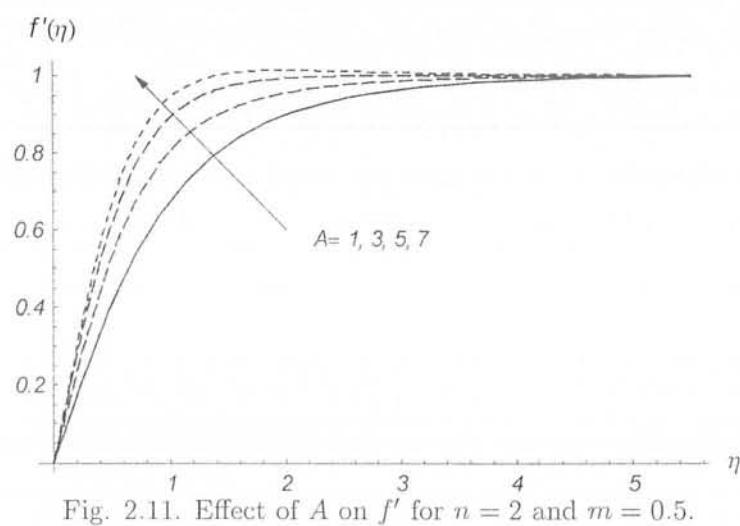
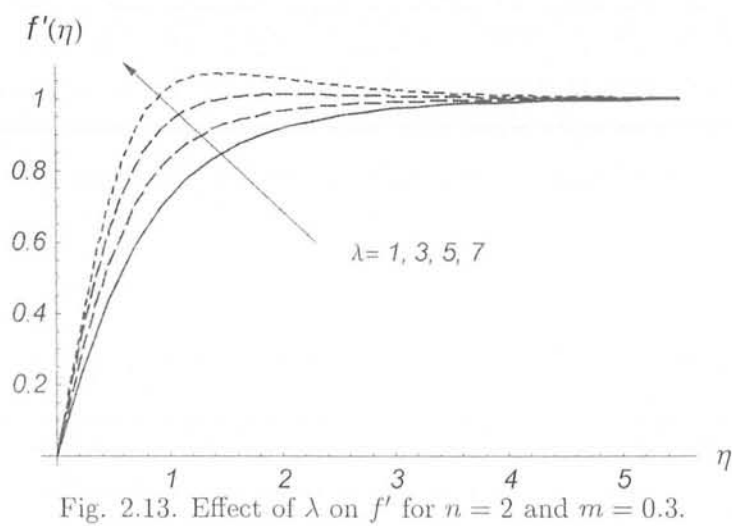
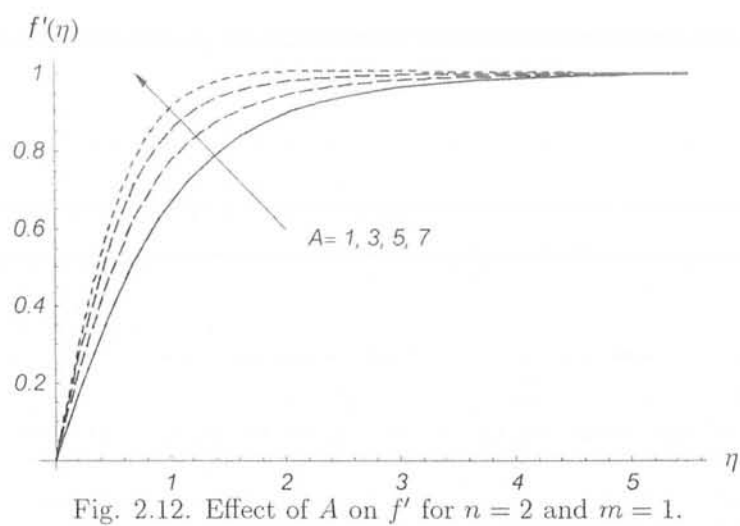


Fig. 2.11. Effect of A on f' for $n = 2$ and $m = 0.5$.



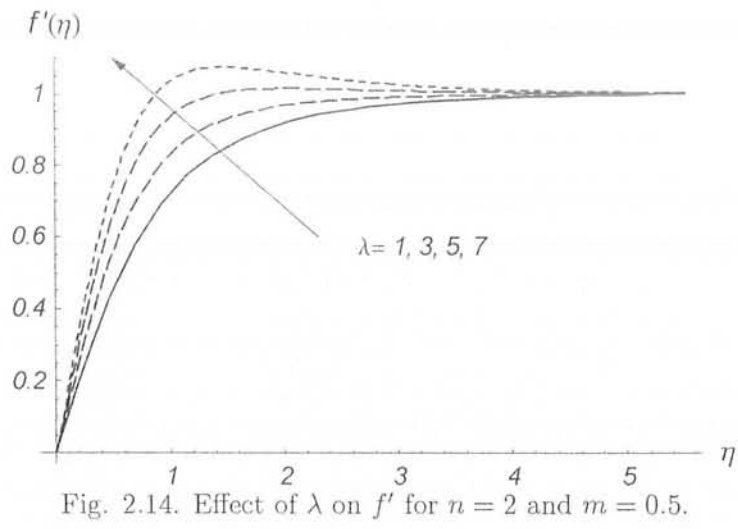


Fig. 2.14. Effect of λ on f' for $n = 2$ and $m = 0.5$.

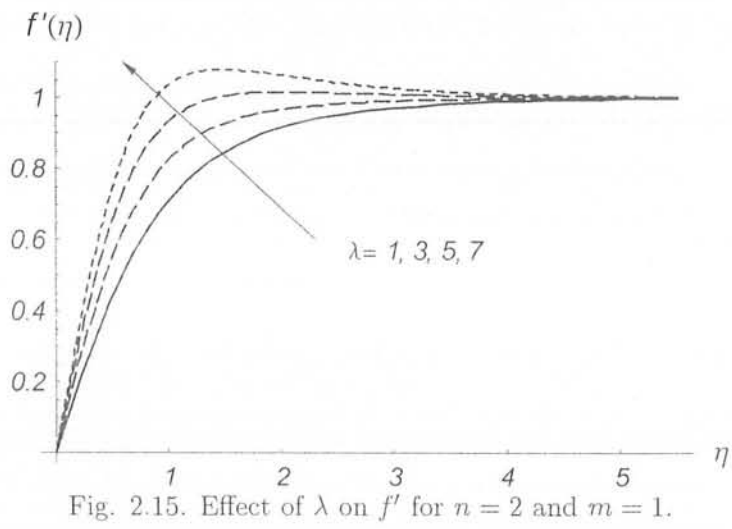


Fig. 2.15. Effect of λ on f' for $n = 2$ and $m = 1$.

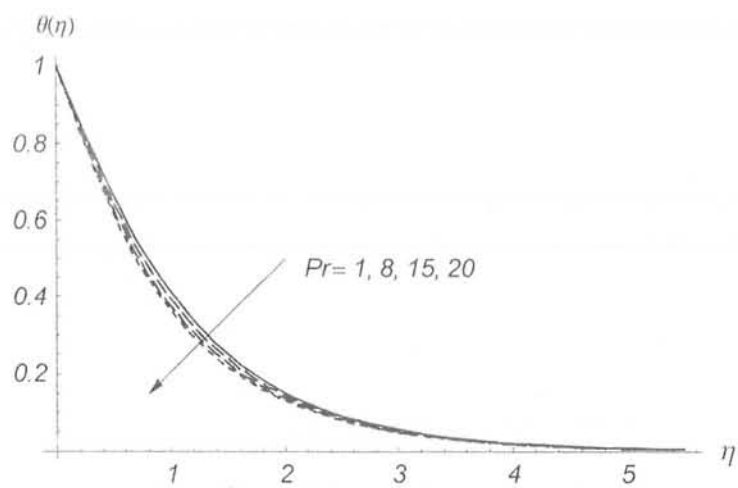


Fig. 2.16. Effect of Pr on θ for $n = 1$ and $m = 0$.

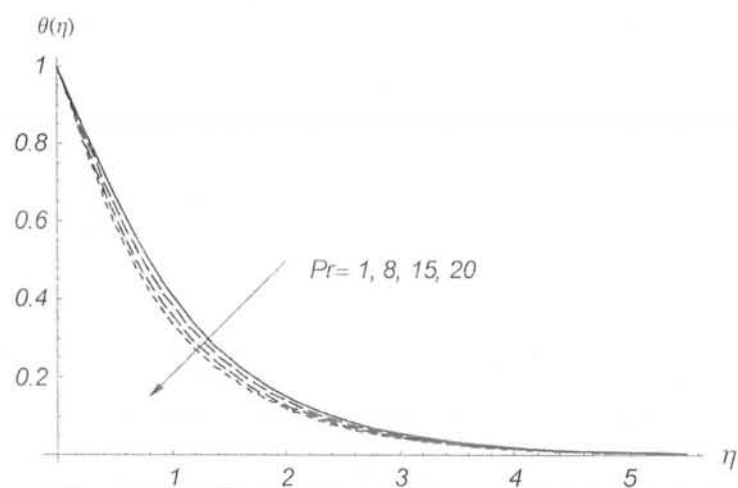


Fig. 2.17. Effect of Pr on θ for $n = 1$ and $m = 0.5$.

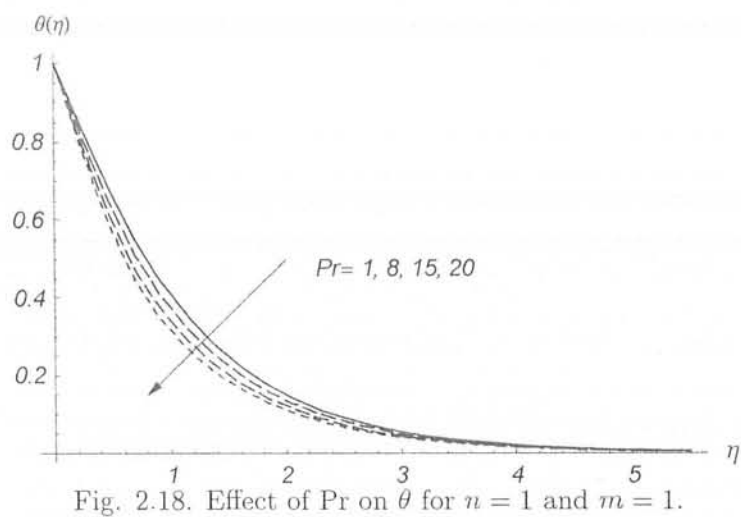


Fig. 2.18. Effect of Pr on θ for $n=1$ and $m=1$.

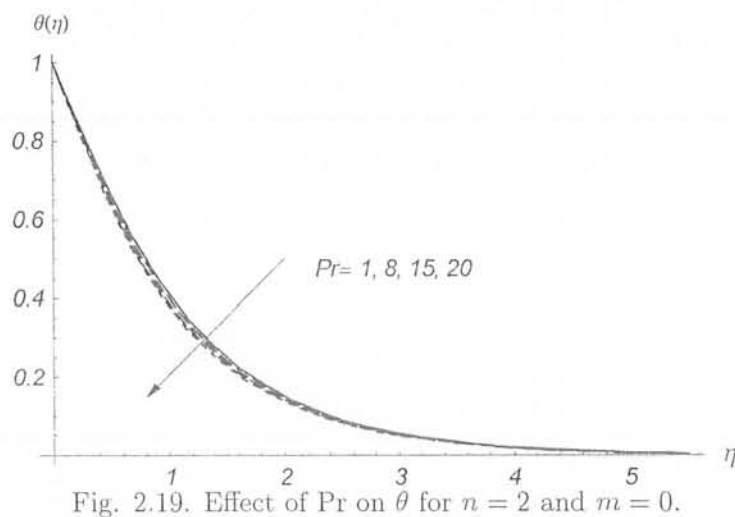


Fig. 2.19. Effect of Pr on θ for $n=2$ and $m=0$.

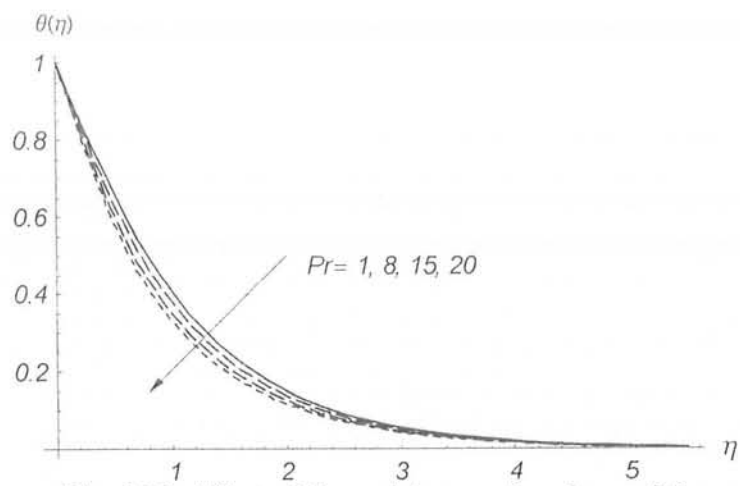


Fig. 2.20. Effect of Pr on θ for $n = 2$ and $m = 0.5$.

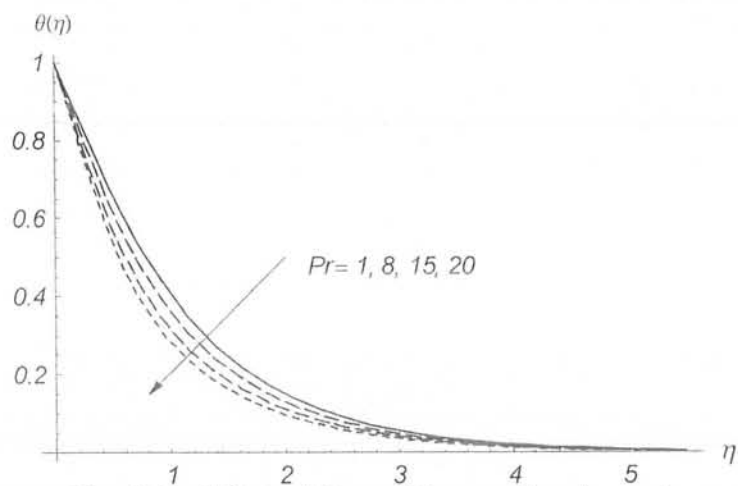


Fig. 2.21. Effect of Pr on θ for $n = 2$ and $m = 1$.

Table. 2.2. Skin friction $(m+1)f''(0)$ for different values of the parameters

m	A	B	λ	α	$(m+1)f''(0)$
0.2	1	0.1	1	$\pi/4$	1.6420
0.5					1.9482
1					2.5582
	0				2.0548
	0.5				2.2792
	1				2.5582
		0			2.4962
		0.5			2.7798
		1			3.0766
0.2		0.1	0.2		1.3062
			0.5		1.4255
			1		1.6420
1			1	$\pi/6$	2.2946
				$\pi/4$	2.5582
				$\pi/2$	2.9192

Table. 2.3. Nusselt number $-\theta'(0)$ for various parameters at $A = 1$, $B = 0.1$, $\lambda = 1$ and $\alpha = \pi/4$.

m	n	Pr	$-\theta'(0)$
0	1	0.1	0.5938
0.5			0.6004
1			0.6011
	1		0.6011
	2		0.6019
	3		0.6083
		0.1	0.6011
		0.6	0.6214
		1.0	0.6326

2.5 Main points

Effect of mixed convection on the Falkner-Skan flow of power-law fluid is investigated. The series solutions are computed by the homotopy analysis method (HAM). The key points of the present analysis are as follows

- Table1 shows that the convergence of the functions f and θ are obtained at 8th-order of approximation.
- Velocity profile increases with the increase of A for both $n = 1$ and $n = 2$.
- Velocity profile increases with an increase in the values of mixed convection parameter λ and boundary layer thickness decreases for $n = 1$ and $n = 2$.
- The influence of Prandtl number (Pr) decreases the temperature profile. It also reduce the thermal boundary thickness for $n = 1$ and $n = 2$.
- The velocity profile increases slowly with the increase of m for the parmater A .
- The velocity profile increases largely with the increase of m for mixed convection parameter λ .
- The temperature profile decreases largely with the increase of m for Prandtl number (Pr).

Chapter 3

Falkner-Skan wedge flow of Maxwell fluid with mixed convection

3.1 Introduction

This chapter consists of the series solution for mixed convection Falkner-Skan flow of an incompressible Maxwell fluid. Analysis has been carried out in the presence of Newtonian heating. Appropriate similarity transformations reduce the nonlinear partial differential equations into nonlinear ordinary differential equations. The series solutions of the present problem is solved by homotopy analysis method (HAM). Convergence of the problem is determined. The effects of different parameters specially Prandtl number (Pr) and conjugate parameter (γ) are shown and discussed. Numerical values of local Nusselt number for different values of (Pr) and (γ) are computed and analyzed.

3.2 Mathematical model

Consider the two-dimensional Falkner-Skan wedge flow of a Maxwell fluid with mixed convection. In this two-dimensional model, the Cartesian coordinates (x, y) are used such that x -axis is parallel to the plate and y -axis normal to it. The fluid occupies the region $y \geq 0$. We assume that the wall is subjected to a Newtonian heating. The continuity, momentum and energy

equations for the Maxwell fluid are given by

$$\nabla \cdot \mathbf{V} = 0, \quad (3.1)$$

$$\rho a = \nabla \cdot \mathbf{T} + \rho g \beta_T (T - T_\infty) \sin \left(\frac{\alpha}{2} \right), \quad (3.2)$$

$$\mathbf{T} = -p\mathbf{I} + \mathbf{S}, \quad (3.3)$$

$$\rho c_p \frac{dT}{dt} = \mathbf{T} \cdot \mathbf{L} - \text{div } \mathbf{q}, \quad (3.4)$$

$$\left(1 + \lambda_1 \frac{D}{Dt} \right) \mathbf{S} = \mu \mathbf{A}_1 \quad (3.5)$$

$$\mathbf{A}_1 = \mathbf{L} + \mathbf{L}^{T*} \quad (3.6)$$

$$\mathbf{q} = -k_0 \text{grad } T, \quad (3.7)$$

and the velocity field is

$$\mathbf{V} = [u(x, y), v(x, y), 0]. \quad (3.8)$$

In the above expressions \mathbf{V} is the velocity, \mathbf{T} is the Cauchy stress tensor, \mathbf{S} is the extra stress tensor, g is the gravitational acceleration which acts in the downward direction, α is the angle of inclination of wedge, ρ is the density of the fluid, c_p is the specific heat at constant pressure, \mathbf{L} is the gradient of velocity, λ_1 is the relaxation time, $\frac{D}{Dt}$ is the covariant derivative, μ is the dynamic viscosity, \mathbf{A}_1 is the first Rivlin-Ericksen tensor, T^* is the transpose, \mathbf{q} is the heat flux, k_0 is the thermal conductivity and T is the temperature of the fluid.

The first Rivlin-Ericksen tensor is

$$\mathbf{A}_1 = \begin{bmatrix} 2\frac{\partial u}{\partial x} & \frac{\partial u}{\partial y} + \frac{\partial v}{\partial x} & 0 \\ \frac{\partial u}{\partial y} + \frac{\partial v}{\partial x} & 2\frac{\partial v}{\partial y} & 0 \\ 0 & 0 & 0 \end{bmatrix}. \quad (3.9)$$

From Eqs. (3.2) and (3.3) we have

$$\rho \left(1 + \lambda_1 \frac{D}{Dt} \right) a = - \left(1 + \lambda_1 \frac{D}{Dt} \right) \nabla p + \mu \nabla \cdot \mathbf{A}_1 + \left(1 + \lambda_1 \frac{D}{Dt} \right) \rho g \beta_T (T - T_\infty) \text{Si } n \left(\frac{\alpha}{2} \right) \quad (3.10)$$

In general form covariant derivative $\frac{D}{Dt}$ can be written as

$$\frac{Da_i}{Dt} = \frac{\partial a_i}{\partial t} + u_j a_{i,j} - u_{i,j} a_j. \quad (3.11)$$

For $i = 1$, the above Eqs. (3.10) and (3.11) become

$$\rho \left(1 + \lambda_1 \frac{D}{Dt} \right) a_1 = - \left(1 + \lambda_1 \frac{D}{Dt} \right) \nabla p + \mu \nabla \cdot \mathbf{A}_1 + \left(1 + \lambda_1 \frac{D}{Dt} \right) \rho g \beta_T (T - T_\infty) \text{Si } n \left(\frac{\alpha}{2} \right) \quad (3.12)$$

and

$$\frac{Da_1}{Dt} = \frac{\partial a_1}{\partial t} + u_1 a_{1,1} + u_2 a_{1,2} - u_{1,1} a_1 - u_{1,2} a_2, \quad (3.13)$$

where a_1 and a_2 are given by

$$a_1 = \frac{du}{dt} = u \frac{\partial u}{\partial x} + v \frac{\partial u}{\partial y}, \quad (3.14)$$

$$a_2 = \frac{dv}{dt} = u \frac{\partial v}{\partial x} + v \frac{\partial v}{\partial y}. \quad (3.15)$$

Using Eqs.(3.13) – (3.15) in Eq. (3.12) we get

$$\begin{aligned} & u \frac{\partial u}{\partial x} + v \frac{\partial u}{\partial y} + \lambda_1 \left[u \frac{\partial}{\partial x} \left(u \frac{\partial u}{\partial x} + v \frac{\partial u}{\partial y} \right) + v \frac{\partial}{\partial y} \left(u \frac{\partial u}{\partial x} + v \frac{\partial u}{\partial y} \right) \right] \\ &= - \frac{1}{\rho} \frac{\partial p}{\partial x} + \nu \left[2 \frac{\partial^2 u}{\partial x^2} + \frac{\partial^2 u}{\partial y^2} + \frac{\partial^2 v}{\partial x \partial y} \right] + g \beta_T (T - T_\infty) \text{Si } n \left(\frac{\alpha}{2} \right). \end{aligned} \quad (3.16)$$

The above equation after using continuity equation can be written as

$$\begin{aligned} & u \frac{\partial u}{\partial x} + v \frac{\partial u}{\partial y} + \lambda_1 \left[u^2 \frac{\partial^2 u}{\partial x^2} + v^2 \frac{\partial^2 u}{\partial y^2} + 2uv \frac{\partial^2 u}{\partial x \partial y} \right] \\ &= -\frac{1}{\rho} \frac{\partial p}{\partial x} + \nu \left[\frac{\partial^2 u}{\partial x^2} + \frac{\partial^2 u}{\partial y^2} \right] + g\beta_T (T - T_\infty) \sin\left(\frac{\alpha}{2}\right). \end{aligned} \quad (3.17)$$

Similarly for $i = 2$, we obtain

$$\begin{aligned} & u \frac{\partial v}{\partial x} + v \frac{\partial v}{\partial y} + \lambda_1 \left[u^2 \frac{\partial^2 v}{\partial x^2} + v^2 \frac{\partial^2 v}{\partial y^2} + 2uv \frac{\partial^2 v}{\partial x \partial y} \right] \\ &= -\frac{1}{\rho} \frac{\partial p}{\partial y} + \nu \left[\frac{\partial^2 v}{\partial x^2} + \frac{\partial^2 v}{\partial y^2} \right] \end{aligned} \quad (3.18)$$

and energy equation (3.4) in the absence of viscous dissipation becomes

$$u \frac{\partial T}{\partial x} + v \frac{\partial T}{\partial y} = \frac{k_0}{\rho c_p} \left(\frac{\partial^2 T}{\partial x^2} + \frac{\partial^2 T}{\partial y^2} \right) \quad (3.19)$$

Now applying the boundary layer approximation to Eqs. (3.1) and (3.17) – (3.19) in which

$$u = O(1), \quad x = O(1), \quad v = O(\delta), \quad y = O(\delta), \quad (3.20)$$

we see that Eq.(3.18) vanishes and Eqs.(3.1), (3.17) and (3.19) are reduced as follows

$$\frac{\partial u}{\partial x} + \frac{\partial v}{\partial y} = 0, \quad (3.21)$$

$$\begin{aligned} & u \frac{\partial u}{\partial x} + v \frac{\partial u}{\partial y} + \lambda_1 \left[u^2 \frac{\partial^2 u}{\partial x^2} + v^2 \frac{\partial^2 u}{\partial y^2} + 2uv \frac{\partial^2 u}{\partial x \partial y} \right] \\ &= -\frac{1}{\rho} \frac{\partial p}{\partial x} + \nu \frac{\partial^2 u}{\partial y^2} + g\beta_T (T - T_\infty) \sin\left(\frac{\alpha}{2}\right), \end{aligned} \quad (3.22)$$

$$u \frac{\partial T}{\partial x} + v \frac{\partial T}{\partial y} = \frac{k}{\rho c_p} \frac{\partial^2 T}{\partial y^2}. \quad (3.23)$$

The boundary conditions are given by

$$\begin{aligned} u &= 0, & v &= 0, & \frac{\partial T}{\partial y} &= -h_s T & \text{at } y = 0, \\ u &\rightarrow U, & T &\rightarrow T_\infty & \text{as } y &\rightarrow \infty, \end{aligned} \quad (3.24)$$

Now Eq. (3.23) becomes

$$\begin{aligned} u \frac{\partial u}{\partial x} + v \frac{\partial u}{\partial y} + \lambda_1 \left[u^2 \frac{\partial^2 u}{\partial x^2} + v^2 \frac{\partial^2 u}{\partial y^2} + 2uv \frac{\partial^2 u}{\partial x \partial y} \right] &= \nu \frac{\partial^2 u}{\partial y^2} + U \frac{\partial U}{\partial x} \\ &+ \lambda_1 U^2 \frac{\partial^2 U}{\partial x^2} + g\beta_T (T - T_\infty) \text{Si } n \left(\frac{\alpha}{2} \right), \end{aligned} \quad (3.25)$$

where $U (= ax^n)$ is the free stream velocity, ρ is the density, λ_1 is the relaxation time and T and T_∞ are the temperatures of the fluid and surrounding respectively.

Let us define the similarity transformations

$$u = U(x) f', \quad \eta = \sqrt{\frac{n+1}{2}} \sqrt{\frac{U}{\nu x}} y, \quad \psi = \sqrt{\frac{2}{n+1}} \sqrt{\nu x U} f(\eta), \quad (3.26)$$

$$v = -\sqrt{\frac{n+1}{2}} \sqrt{\frac{\nu U}{x}} \left[f(\eta) + \frac{n-1}{n+1} \eta f'(\eta) \right], \quad \theta(\eta) = \frac{T - T_\infty}{T_\infty}. \quad (3.27)$$

Using these transformations, Eq. (3.21) is identically satisfied and Eqs. (3.23) – (3.24) become

$$f''' + f f'' + \beta_1 \left(2n \left(\frac{n-1}{n+1} \right) (1 - f'^3) + (3n-1) f f' f'' \right) + \frac{2n}{n+1} (1 - f'^2) + \lambda \theta \text{Si } n \left(\frac{\alpha}{2} \right) = 0, \quad (3.28)$$

$$\theta'' + \text{Pr } f \theta' = 0, \quad (3.29)$$

$$\begin{aligned} f(0) &= f'(0) = 0, & \theta'(0) &= -\gamma [1 + \theta(0)], \\ f'(\infty) &= 1, & \theta(\infty) &= 0, \end{aligned} \quad (3.30)$$

in which prime denotes the differentiation with respect to η , Pr is the Prandtl number, β_1 is the dimensionless Deborah number, λ is the mixed convection parameter, γ is the conjugate

parameter and Gr_x is the local Grashof number. These dimensionless quantities are defined by

$$\text{Pr} = \frac{\mu c_p}{k}, \quad \beta_1 = \frac{\lambda_1 U}{x}, \quad \lambda = \frac{Gr_x}{\text{Re}^2}, \quad \gamma = h_s \sqrt{\frac{2\nu x}{(n+1)U}}, \quad Gr_x = \frac{(n+1)g\beta_T T_\infty x^3}{2\nu^2}. \quad (3.31)$$

The local Nusselt number Nu_x is defined as

$$Nu_x = \frac{xq_w}{k_0(T - T_\infty)}, \quad (3.32)$$

where

$$q_w = -k_0 \left(\frac{\partial T}{\partial y} \right)_{y=0}. \quad (3.33)$$

The Nusselt number after using the similarity transformation becomes

$$(\text{Re}_x)^{-1/2} Nu_x = \gamma \left(1 + \frac{1}{\theta(0)} \right), \quad (3.34)$$

where $\text{Re}_x = xU(n+1)/2\nu$ is the local Reynolds number.

3.3 Solutions by homotopy analysis method (HAM)

The initial guesses and auxiliary linear operators are of the following forms

$$f_0(\eta) = \eta - \frac{1 - \exp(-2\eta)}{2}, \quad \theta_0(\eta) = \frac{\gamma}{1-\gamma} e^{-\eta} \quad \gamma \neq 1, \quad (3.35)$$

$$\mathcal{L}_f(f) = \frac{d^3 f}{d\eta^3} - \frac{df}{d\eta}, \quad \mathcal{L}_\theta(f) = \frac{d^2 f}{d\eta^2} - f, \quad (3.36)$$

with the properties

$$\mathcal{L}_f[A_1 + A_2 \exp(\eta) + A_3 \exp(-\eta)] = 0, \quad (3.37)$$

$$\mathcal{L}_\theta[A_4 \exp(\eta) + A_5 \exp(-\eta)] = 0, \quad (3.38)$$

in which A_i ($i = 1 - 5$) are the arbitrary constants.

3.3.1 Zeroth order problem

$$(1-q) \mathcal{L}_f [\widehat{f}(\eta; q) - f_0(\eta)] = q \hbar_f \mathcal{N}_f [\widehat{f}(\eta; q)], \quad (3.39)$$

$$(1-q) \mathcal{L}_\theta [\widehat{\theta}(\eta; q) - \theta_0(\eta)] = q \hbar_\theta \mathcal{N}_\theta [\widehat{\theta}(\eta; q), \widehat{f}(\eta; q)], \quad (3.40)$$

$$\widehat{f}(0; q) = 0, \quad \widehat{f}'(0; q) = 0, \quad \widehat{f}'(\infty; q) = 1, \quad (3.41)$$

$$\widehat{\theta}'(0; q) = -\gamma (1 + \widehat{\theta}(0; q)), \quad \widehat{\theta}(\infty; q) = 0, \quad (3.42)$$

where $q \in [0, 1]$ is the embedding parameter, \hbar_f and \hbar_θ are the non-zero auxiliary parameters and \mathcal{N}_f and \mathcal{N}_θ are the nonlinear operators. We define

$$\begin{aligned} \mathcal{N}_f (\widehat{f}(\eta, q), \widehat{\theta}(\eta; q)) &= \frac{\partial^3 f(\eta; q)}{\partial \eta^3} + f(\eta; q) \frac{\partial^2 f(\eta; q)}{\partial \eta^2} + \frac{2n}{n+1} \left(1 - \left(\frac{\partial f(\eta; q)}{\partial \eta} \right)^2 \right) \\ &+ \beta_1 \left(2n \frac{n-1}{n+1} \left(1 - \left(\frac{\partial f(\eta; q)}{\partial \eta} \right)^3 \right) + (3n-1) f(\eta; q) \frac{\partial f(\eta; q)}{\partial \eta} \frac{\partial^2 f(\eta; q)}{\partial \eta^2} \right. \\ &\quad \left. - \frac{n+1}{2} (f(\eta; q))^2 \frac{\partial^3 f(\eta; q)}{\partial \eta^3} + \frac{n-1}{2} \eta \left(\frac{\partial f(\eta; q)}{\partial \eta} \right)^2 \frac{\partial^2 f(\eta; q)}{\partial \eta^2} \right) + \lambda \theta \operatorname{Si} n \left(\frac{\alpha}{2} \right) \end{aligned} \quad (3.43)$$

$$\mathcal{N}_\theta [\widehat{\theta}(\eta; q), \widehat{f}(\eta; q)] = \frac{\partial^2 \widehat{\theta}(\eta; q)}{\partial \eta^2} + \operatorname{Pr} \widehat{f}(\eta; q) \frac{\partial \widehat{\theta}(\eta; q)}{\partial \eta}. \quad (3.44)$$

3.3.2 m th-order deformation problems

$$\mathcal{L}_f [f_m(\eta) - \chi_m f_{m-1}(\eta)] = \hbar_f \mathcal{R}_m^f(\eta), \quad (3.45)$$

$$\mathcal{L}_\theta [\theta_m(\eta) - \chi_m \theta_{m-1}(\eta)] = \hbar_\theta \mathcal{R}_m^\theta(\eta), \quad (3.46)$$

$$f_m(0) = f'_m(0) = f'_m(\infty) = f''_m(\infty) = 0, \quad (3.47)$$

$$\theta'_m(0) + \gamma \theta_m(0) = \theta_m(\infty) = 0, \quad (3.48)$$

$$\begin{aligned} \mathcal{R}_m^f(\eta) &= f'''_{m-1}(\eta) + \sum_{k=0}^{m-1} \left[f_{m-1-k} f''_k - \frac{2n}{n+1} f'_{m-1-k} f'_k + \beta_1 \left(\begin{aligned} &-2n \frac{n-1}{n+1} f'_{m-1-k} \sum_{l=0}^k f'_{k-l} f'_l \\ &+ (3n-1) f_{m-1-k} \sum_{l=0}^k f'_{k-l} f''_l \\ &- \frac{n+1}{2} f_{m-1-k} \sum_{l=0}^k f_{k-l} f'''_l \\ &+ \frac{n-1}{2} \eta f'_{m-1-k} \sum_{l=0}^k f'_{k-l} f''_l \end{aligned} \right) \right. \\ &\quad \left. + \lambda \theta_{m-1} \operatorname{Si} n \left(\frac{\alpha}{2} \right) + \frac{2n}{n+1} [1 + \beta_1 (n-1)] (1 - \chi_m) \right], \end{aligned} \quad (3.49)$$

$$\mathcal{R}_m^\theta(\eta) = \theta''_{m-1} + \Pr \sum_{k=0}^{m-1} \theta'_{m-1-k} f_k, \quad (3.50)$$

$$\chi_m = \begin{cases} 0, & m \leq 1 \\ 1, & m > 1 \end{cases}. \quad (3.51)$$

If $q = 0$ and $q = 1$, then

$$\widehat{f}(\eta; 0) = f_0(\eta), \quad \widehat{f}(\eta; 1) = f(\eta), \quad (3.52)$$

$$\widehat{\theta}(\eta; 0) = \theta_0(\eta), \quad \widehat{\theta}(\eta; 1) = \theta(\eta) \quad (3.53)$$

By virtue of above equations, when q increases from 0 to 1 then $\widehat{f}(\eta; q)$ and $\widehat{\theta}(\eta; q)$ vary from $f_0(\eta)$ and $\theta_0(\eta)$ to $f(\eta)$ and $\theta(\eta)$ respectively. Here \hbar is the nonzero auxiliary parameter. By Taylor's theorem and Eqs. (3.52) and (3.53), we have

$$\widehat{f}(\eta; q) = f_0(\eta) + \sum_{m=1}^{\infty} f_m(\eta) q^m, \quad f_m(\eta) = \frac{1}{m!} \left. \frac{\partial^m \widehat{f}(\eta; q)}{\partial q^m} \right|_{q=0} \quad (3.54)$$

$$\widehat{\theta}(\eta; q) = \theta_0(\eta) + \sum_{m=1}^{\infty} \theta_m(\eta) q^m, \quad \theta_m(\eta) = \frac{1}{m!} \left. \frac{\partial^m \widehat{\theta}(\eta; q)}{\partial q^m} \right|_{q=0}, \quad (3.55)$$

where the auxiliary parameters are so properly chosen that the series (3.54) and (3.55) converge at $q = 1$ i.e.

$$f(\eta) = f_0(\eta) + \sum_{m=1}^{\infty} f_m(\eta), \quad (3.56)$$

$$\theta(\eta) = \theta_0(\eta) + \sum_{m=1}^{\infty} \theta_m(\eta). \quad (3.57)$$

The general solutions of Eqs. (3.45) and (3.46) are

$$f_m(\eta) = f_m^*(\eta) + A_1 + A_2 e^\eta + A_3 e^{-\eta}, \quad (3.58)$$

$$\theta_m(\eta) = \theta_m^*(\eta) + A_4 e^\eta + A_5 e^{-\eta}, \quad (3.59)$$

where $f_m^*(\eta)$ and $\theta_m^*(\eta)$ are the special solutions and the values of A_i ($i = 1 - 5$) along with the boundary conditions (3.47) and (3.48) are

$$\begin{aligned} A_2 &= A_4 = 0, & A_3 &= \left. \frac{\partial f_m^*(\eta)}{\partial \eta} \right|_{\eta=0}, & A_1 &= -A_3 - f_m^*(0), \\ A_5 &= \frac{1}{1-\gamma} \left(\left. \theta_m^{*'}(\eta) \right|_{\eta=0} + \gamma \theta_m^*(\eta) \right|_{\eta=0} \right), \end{aligned} \quad (3.60)$$

Note that the solutions of the problems involving Eqs. (3.45) – (3.51) have been developed by using the symbolic computation software MATHEMATICA when $m = 1, 2, 3, \dots$

3.4 Solution analysis

3.4.1 Convergence of the series solutions

We know that the series solutions given in Eqs. (3.56) and (3.57) have auxiliary parameters \hbar_f and \hbar_θ . As pointed out by Liao, the convergence of the series solutions is highly dependent upon these parameters. For the determination of a valid range for values of these parameters, we have sketched the \hbar -curves at 20th-order of approximations (see Fig. 3.2 and 3.3). These Figs. show that the admissible ranges of values of \hbar_f and \hbar_θ are $-1.4 \leq \hbar_f \leq -0.65$ and $-1.6 \leq \hbar_\theta \leq -0.7$. Further Table 1 ensures that the series solutions are convergent up to five decimal places.

3.4.2 Result and discussion

The aim of this section is to describe the variation of embedded parameters on the velocity, temperature and surface heat transfer. Fig. 3.3 is plotted for velocity profiles for various values of Deborah number β_1 . It is observed that velocity field increases when β_1 increases. Figs. 3.4 and 3.5 show the effects of mixed convection parameter λ and n . These Figs. show that by increasing the values of mixed convection parameter λ and n , there is a gradual increase in the velocity profile. Further the boundary layer thickness is reduced. The effects of Prandtl number Pr and conjugate parameter γ on velocity profile are presented in the Figs. 3.6 and 3.7. It is noted that an increase in the values of Pr and γ increases the velocity profile while such increase reduces the thermal boundary layer thickness. The effect of Prandtl number Pr on θ can be

visualized in Fig. 3.8. It is obvious that an increase in the values of Pr greatly reduces the thermal diffusivity, and consequently the temperature and the thermal boundary layer thickness are decreasing functions of Pr . It is also observed that deviation in the temperature profiles are more significant for small values of Pr when compared with its larger values. The influence of conjugate parameter γ on the velocity profile is displayed in Fig. 3.9. As expected, the larger values of γ accompany with the higher Newtonian heating which increases the temperature and the thermal boundary layer thickness. An increase in n corresponds to a decrease in the temperature and the thermal boundary layer thickness (see Fig. 3.10). To capture the effects of inclination angle α on the velocity f' we have plotted Fig. 3.11. It is depicted that velocity increases and the boundary layer thickness is decreasing function of α .

The study of Table 1 indicates that 20th-order approximation gives a convergent series solution. Numerical values of local Nusselt number for various values of parameters are computed in Table 2. It is noticed that local Nusselt number is an increasing function of Pr and γ .

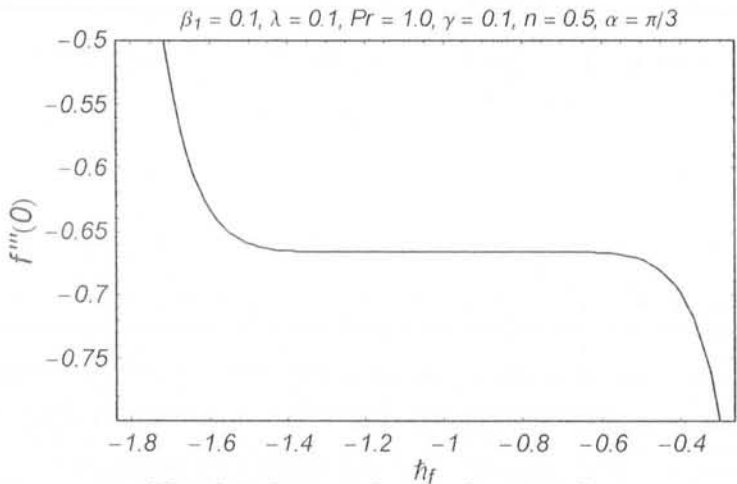


Fig. 3.1. h -curve for the function f .

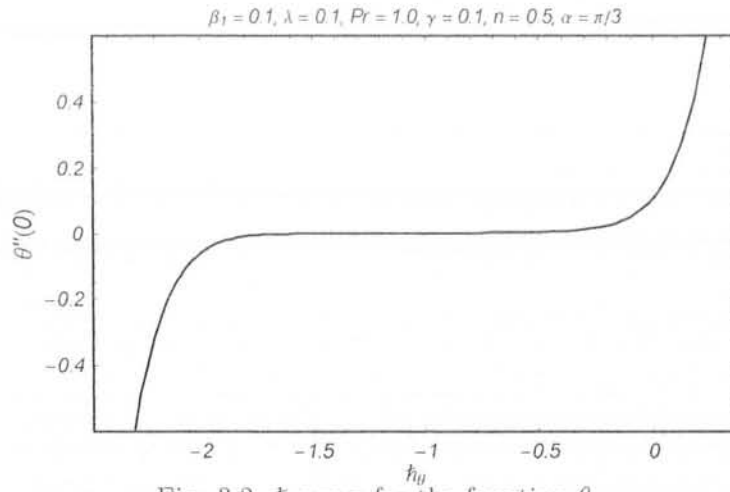


Fig. 3.2. h -curve for the function θ .

Table 3.1 : Convergence of the homotopy solutions for different order of approximation when $Pr = 1.0$, $\lambda = 0.1$, $n = 0.5$, $\beta_1 = 0.1$, $\alpha = \pi/3$, $\gamma = 0.1$ and $h_f = h_\theta = -0.8$.

Order of approximation	$-f'''(0)$	$\theta''(0)$
5	0.756033	0.0138966
10	0.657312	0.0058769
15	0.655760	0.0037962
20	0.655961	0.0035451
25	0.655961	0.0035451
30	0.655961	0.0035451

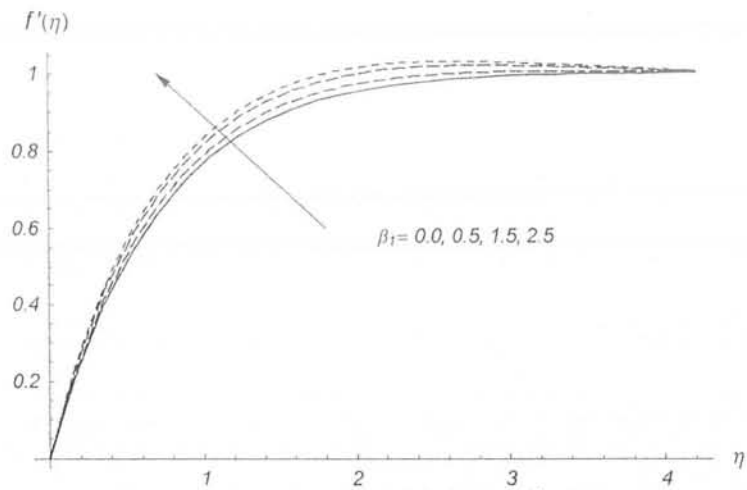


Fig. 3.3: Effect of β_1 on f' .

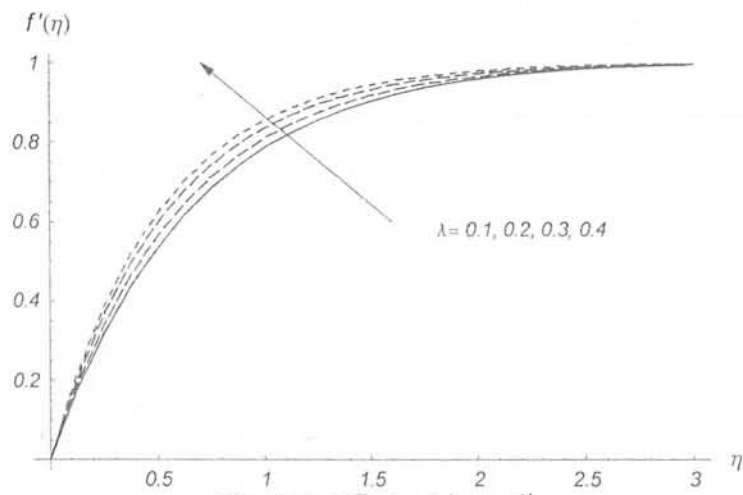


Fig. 3.4: Effect of λ on f' .

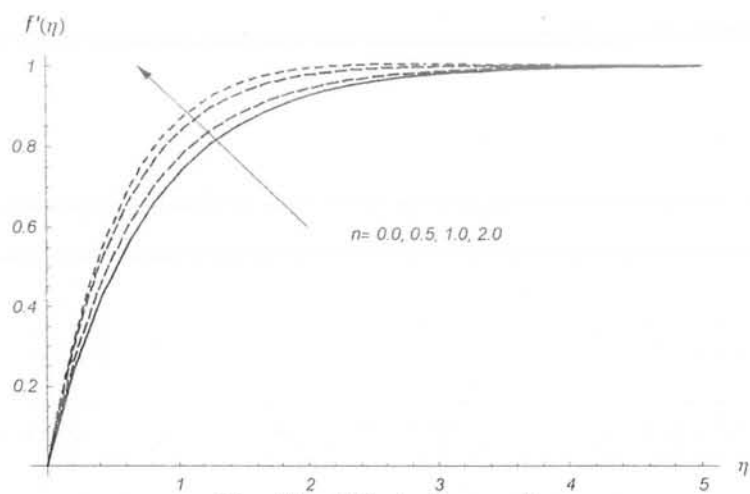


Fig. 3.5: Effect of n on f' .

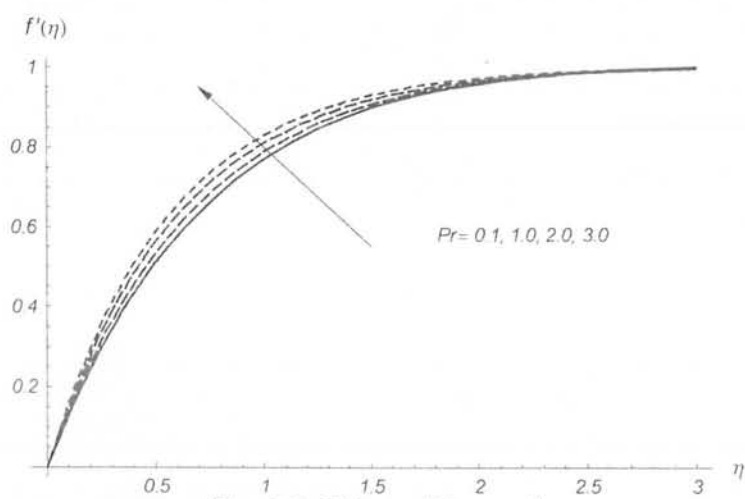


Fig. 3.6: Effect of Pr on f' .

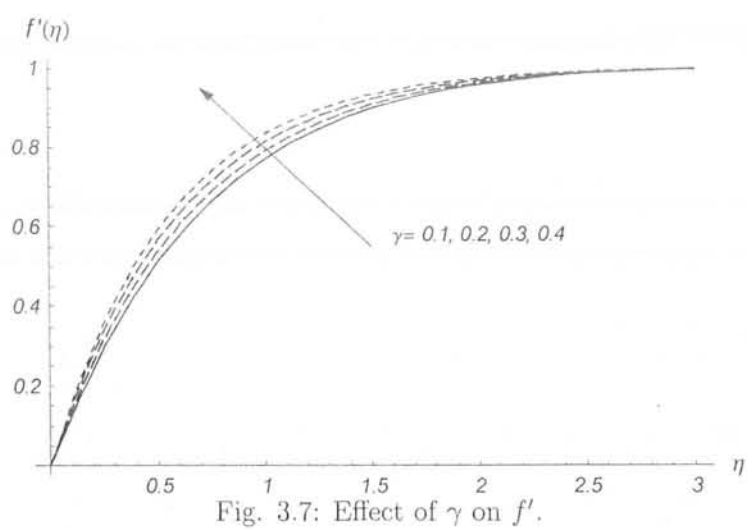


Fig. 3.7: Effect of γ on f' .

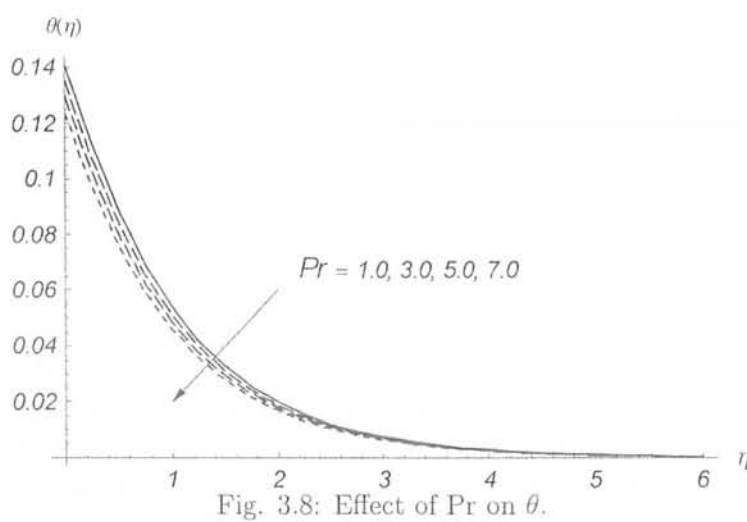
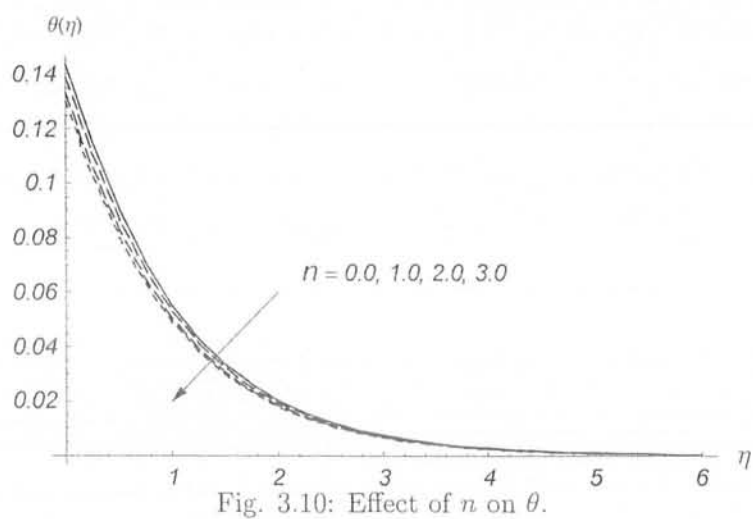
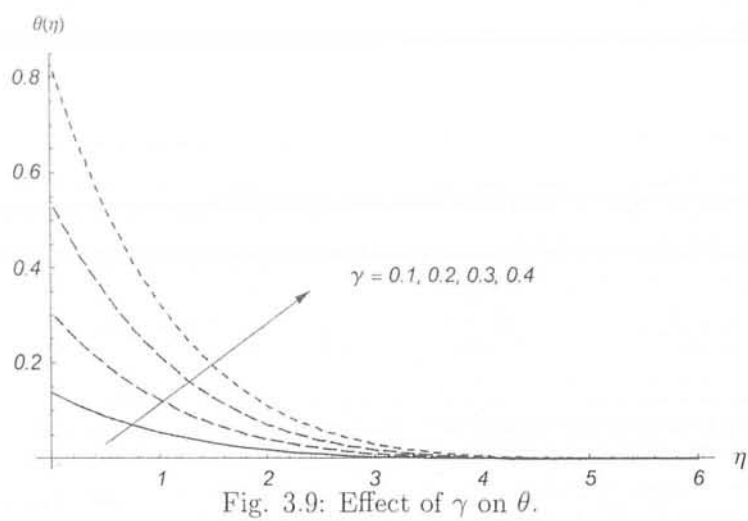


Fig. 3.8: Effect of Pr on θ .



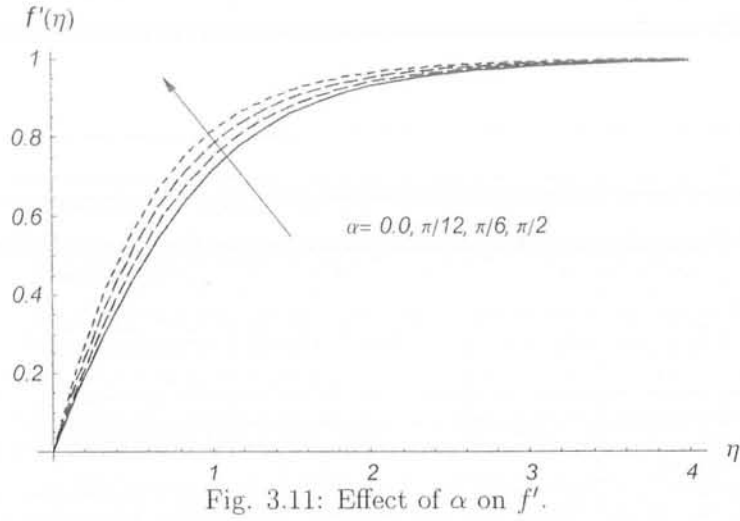


Table 3.2: Values of $(\text{Re}_x)^{-1/2} Nu_x$ for different values of Pr and γ when $\beta_1 = \lambda = 0.1$, $\alpha = \pi/3$ and $h_f = h_\theta = -0.8$

Pr	γ	$-(\text{Re}_x)^{-1/2} Nu_x$
0.5	0.1	0.6637
1.0		0.6733
1.2		0.6822
2.0		0.7025
1.0	0.1	0.6733
	0.2	0.6821
	0.3	0.6925
	0.4	0.6940

3.5 Conclusions

The effects of Newtonian heating on the mixed convection Falkner-Skan flow of Maxwell fluid are described. The arising nonlinear problem is computed. The presented analysis show the following key points.

- Table 1 reveals that convergence of the functions f and θ are obtained at 20th-order

approximations up to five decimal places when $h_f = h_\theta = -0.8$.

- The conjugate parameter γ appreciably increases the dimensionless temperature and surface heat transfer.
- The fluid parameter β_1 increases the velocity whereas the boundary layer thickness decreases.
- The influence of Prandtl number Pr decreases the temperature and the thermal boundary layer thickness.
- The mixed convection parameter λ increases the velocity and decreases the velocity boundary layer thickness.

Bibliography

- [1] C. Fetecau, M. Mahmood and M. Jamil, Exact solutions for the flow of a viscoelastic fluid induced by a circular cylinder subject to a time dependent shear stress, *Comm. Non-linear Sci. Numer. Simul.* 15 (2010) 3931 – 3938.
- [2] T. Hayat, M. Qasim and Z. Abbas, Radiation and mass transfer effects on the magneto-hydrodynamic unsteady flow induced by a stretching sheet, *Z. Naturforsch* 65 (2010) 231 – 239.
- [3] T. Hayat, M. Mustafa and S. Mesloub, Mixed convection boundary layer flow over a stretching surface filled with a Maxwell fluid in presence of Soret and Dufour effects, *Z. Naturforsch.* 65a (2010) 401 – 410.
- [4] R. Cortell, Suction, viscous dissipation and thermal radiation effects on the flow and heat transfer of a power-law fluid past an infinite porous plate, *Chem. Eng. Res. Des.* 89 (2011) 85 – 93.
- [5] L. Zheng, F. Zhao and X. Zhang, Exact solutions for generalized Maxwell fluid flow due to oscillatory and constantly accelerating plate, *Nonlinear Anal. : RWA.* 11 (2010) 3744–3751.
- [6] S. Wang and W. C. Tan, Stability analysis of double-diffusive convection of Maxwell fluid in a porous medium heated from below, *Phys. Lett. A.* 372 (2008) 3046 – 3050.
- [7] S. Abbasbandy and T. Hayat, Solution of the MHD Falkner-Skan flow by Hankel-Pade method, *Phys. Lett. A.* 373 (2009) 731 – 734.
- [8] T. Fang and J. Zhang, An exact analytic solution of the Falkner-Skan equation with mass transfer and wall stretching, *Int. J. Non-Linear Mech.* 43 (2008) 1000 – 1006.

- [9] B. Yao, Approximate analytic solution of the Falkner-Skan wedge flow with permeable of uniform suction, *Comm. Non-linear Sci. Numer. Simul.* 14 (2009) 3320 – 3326.
- [10] T. Hayat, M. Hussain, S. Nadeem and S. Mesloub, Falkner–Skan wedge flow of a power-law fluid with mixed convection and porous medium, *Computer and Fluids*, 49 (1) (2011) 22 – 28.
- [11] S. Srinivas and R. Muthuraj, Effects of thermal radiation and space porosity on MHD mixed convection flow in a vertical channel using homotopy analysis method, *Comm. Nonlinear. Sci. Numer. Simulat.* 15 (2010) 2098 – 2108.
- [12] I. Muhaimin, R. Kandasamy and I. Hashim, Thermophoresis and chemical reaction effects on non-Darcy MHD mixed convection heat and mass transfer past a porous wedge in the presence of variable stream condition. *Chem. Eng. Research Design.* 87 (2009) 1527 – 1535.
- [13] T. Hayat, M. Mustafa and I. Pop, Heat and mass transfer for Soret and Dufour's effect on mixed convection boundary layer flow over a stretching vertical surface in a porous medium filled with a viscoelastic fluid, *Comm. Nonlinear. Sci. Numer. Simulat.* 15 (2010) 1183 – 1196.
- [14] O. Aydın and A. Kaya, Mixed convection of a viscous dissipating fluid about a vertical flat plate, *Applied Mathematical Modelling*, 31 (2010) 843 – 853.
- [15] J. H. Merkin, Natural-Convection Boundary-Layer Flow on a Vertical Surface with Newtonian Heating, *Int. J. Heat Fluid Flow*, 15 (1994) 392 – 398.
- [16] M. Z. Salleh, R. Nazar and I. Pop, Forced convection boundary layer flow at a forward stagnation point with Newtonian heating, *Chem. Eng. Commun.* 196 (2009) 987 – 996.
- [17] M. Z. Salleh, R. Nazar and I. Pop, Mixed convection boundary layer flow over a horizontal circular cylinder with Newtonian heating, *Heat Mass Transfer* 46 (2010) 1411 – 1418.
- [18] M. Z. Salleh and R. Nazar, Free convection boundary layer flow over a horizontal circular cylinder with Newtonian heating, *Sains Malays.* In press (2010).

- [19] D. Lesnic, D. B. Ingham and I. Pop, Free convection boundarylayer flow along a vertical surface in a porous medium with Newtonian heating, *Int. J. Heat Mass Transfer.* 42 (1999) 2621 – 2627.
- [20] I. Pop, D. Lesnic and D. B. Ingham, Asymptotic solutions for the free convection boundary-layer flow along a vertical surface in a porous medium with newtonian heating, *Hybrid Meth. Eng.* 2 (2000) 31.
- [21] R. C. Chaudhary and P. Jain, An exact solution to the unsteady free convection boundary layer flow past an impulsive started vertical surface with Newtonian heating , *J. Eng. Phys.* 80 (2007) 954 – 960.
- [22] S. J. Liao, *Beyond perturbation: introduction to the homotopy analysis method.* CRC press LLC; 2004.
- [23] S. Abbasbandy and T. Hayat, On series solution for unsteady boundary layer equations in a special third grade fluid. *Comm. Nonlinear Sci. Num. Simul.* 16 (2011) 3140 – 3146.
- [24] M. M. Rashidi and S. A. M. Pour, Analytic approximate solutions for unsteady boundary-layer flow and heat transfer due to a stretching sheet by homotopy analysis method, *Non-linear Analysis: Modelling and Control*, 15(1) (2010) 83 – 95.
- [25] T. Hayat, M. Qasim and Z. Abbas, Homotopy solution for unsteady three-dimensional MHD flow and mass transfer in a porous space. *Comm. Nonlinear. Sci. Numer. Simulat.* 15 (2010) 2375 – 2387.
- [26] B. Yao, Series solution of the temperature distribution in the Falkner-Skan wedge flow by the homotopy analysis method, *Euro. J. Mech. B/ Fluids.* 28 (2009) 689 – 693.
- [27] C. S. Liu, The essence of the homotopy analysis method, *Appl. Math. Comp* 216 (2010) 1299 – 1303.
- [28] J. Cheng, S. Liao, R. N. Mohapatra and K. Vajravelu, Series solutions of nano boundary layer flows by means of the homotopy analysis method, *J. Math. Anal. Appl.* 343 (2008) 233 – 245.